Yugoslav Journal of Operations Research
xx (20xx), Number xx, xxx–xxx
DOI: https://doi.org/10.2298/YJOR250715043H

Research Article

MULTI-OBJECTIVE MULTI-PERIOD FACILITY COVERING LOCATION AND CAPACITY PLANNING WITH MULTIPLE ROOT FACILITIES UNDER UNCERTAINTY

Girma HAILEMARIAM*
Department of Mathematics, Arba Minch University, Arba Minch, Ethiopia
gghnb1357@gmail.com, ORCID: 0009-0001-7461-7922

Natesan THILLAIGOVINDAN
Department of Mathematics,Arba Minch University, Arba Minch, Ethiopia
thillaigovindan.natesan@gmail.com, ORCID: 0000-0002-3710-8918

Getenet ALEMAYHU
Department of Mathematics, Haramaya University, Harar, Ethiopia
getalem2014@gmail.com, ORCID:0000-0002-1561-2996

Received: July 2025 / Accepted: November 2025

Abstract: This strategic planning framework is built upon a Multi-Objective Optimization core, balancing cost efficiency, service coverage, equity, and environmental impact. This core is intrinsically linked to Multi-Period Planning, which handles phased investment, capacity expansion, and network adaptation over time. To address real-world variability, Uncertainty Management techniques such as modeling stochastic demand, scenario-based planning, and service level constraints are integrated directly into the multi-period model. Finally, the physical and logical layout is governed by key Network Design Considerations, including the use of shortest path forests, multiple root facilities, modular capacity units, and resilience measures to ensure robust operation.

Keywords: Facility location, capacity planning, stochastic optimization, network design, multi-objective programming, interconnection cost minimization.

*Corresponding author

MSC: 90C29, 90C15.

1. INTRODUCTION

Facility location problems (FLPs) constitute a fundamental class of optimization challenges with critical applications across public health infrastructure, logistics networks, emergency services, and sustainable energy systems. These problems focus on determining optimal spatial configurations of facilities to efficiently serve distributed demand populations, a research domain that has evolved significantly since Weber's pioneering work on industrial location theory [1] and Hakimi [2] on network theory. While substantial theoretical and methodological advances have been achieved, the escalating complexity of real-world planning environments continues to present challenges that existing approaches address only partially. Traditional facility location models, including the classical p-median [3] and p-center [4] formulations, were primarily designed for static, single-period decision-making with deterministic parameters and single objectives. Although these models provided valuable foundational frameworks, their simplifying assumptions often prove inadequate for addressing the dynamic, uncertain, and multi-faceted nature of contemporary planning challenges. Modern facility location decisions must simultaneously accommodate temporal dynamics through multi-period planning horizons, contend with uncertainty in demand and resource availability, balance multiple competing objectives including cost efficiency and service equity, and consider complex network structures and connectivity requirements [5, 6].

The evolution of FLP research has progressed along several specialized trajectories in response to these challenges. Multi-period planning frameworks enable phased investment strategies that adapt to changing system conditions [7, 8]. Uncertainty management approaches, including stochastic programming [9, 10] and distributionally robust optimization [11], handle unpredictable demand patterns and resource availability. Multi-objective optimization techniques have advanced from simple weighted-sum approaches to sophisticated Pareto-based methods that explicitly address trade-offs between competing criteria [12, 13]. Network design considerations have evolved to include hierarchical structures, resilience measures, and innovative concepts such as shortest path forests with multiple root facilities [14, 15]. Recent advancements in exact solution approaches, such as the AUGMECON-R method, enable systematic Pareto frontier construction by reformulating multi-objective problems into augmented ε-constraint models, ensuring both computational efficiency and strong theoretical guarantees. Complementing this, specialized metaheuristics such as the proposed AugForestExplorer method have been developed to efficiently explore large-scale instances of shortest path forest structures, combining heuristic exploration with Pareto-based evaluation to overcome scalability barriers.

Despite these significant advances within individual research streams, a critical gap persists in the literature: the absence of integrated frameworks that simultaneously address the interconnected challenges of multi-period planning, uncertainty management, multi-objective optimization, and network design. Most existing approaches address only subsets of these dimensions, potentially overlooking important interactions and synergies between different complexity sources. This fragmentation limits the practical applicability of current models to real-world problems that inherently involve all these di-

mensions concurrently. This paper addresses these research gaps by introducing a comprehensive Multi-Objective Multi-Period Capacity Planning in Covering Location Problems with Multiple Roots and Shortest Path Forest under Uncertainty (MMFLCP-MRFU) framework. Our approach integrates multiple dimensions of facility location complexity within a unified modeling paradigm, specifically incorporating multi-period planning with phased investment decisions, uncertainty management through scenario-based stochastic programming, multi-objective optimization balancing cost efficiency and service coverage, and network design features including shortest path forests with multiple root facilities. The integration of AUGMECON-R for exact Pareto frontier generation and AugForestExplorer for scalable heuristic search represents a methodological advancement that significantly enhances both solution quality and computational tractability.

This research addresses the problem of optimally locating and configuring facilities within networked systems under uncertainty, where decisions must balance multiple competing objectives across extended time horizons while ensuring efficient connectivity through shortest path forest structures. The problem is particularly relevant for critical infrastructure planning in sectors such as healthcare and renewable energy, where strategic decisions have long-term consequences and must accommodate evolving demand patterns, budget constraints, and sustainability requirements. The relevance of this research stems from its direct applicability to pressing real-world challenges in infrastructure planning and resource allocation. As societies face increasing pressures from urbanization, climate change, and public health crises, the need for robust facility location frameworks that can handle complexity and uncertainty becomes increasingly critical. Our integrated approach provides decision-makers with practical tools for designing resilient service networks that can adapt to changing conditions while maintaining efficiency and equity. The novelty and contributions of this work are substantial and multifaceted. First, we introduce the integrated framework that simultaneously addresses multi-period planning, demand uncertainty, multi-objective optimization, and complex network design with multiple roots within a unified modeling structure. This represents a significant advancement over existing approaches that typically address these dimensions in isolation. Second, we develop a novel two-stage stochastic mixed-integer programming formulation that captures the intricate interplay between strategic facility location decisions and operational allocation choices under uncertainty. Third, we propose innovative solution methodologies combining exact optimization techniques such as AUGMECON-R with specialized metaheuristics such as AugForestExplorer to handle the computational complexity of the integrated model. Finally, we demonstrate the practical utility of our framework through comprehensive case studies in healthcare and energy sectors, providing valuable insights for both researchers and practitioners.

The principal contributions of this work are fourfold. First, we develop an integrated modeling framework that simultaneously addresses multiple dimensions of facility location complexity typically treated in isolation. Second, we propose a novel two-stage stochastic mixed-integer linear programming formulation capturing the interplay between strategic facility location decisions and operational allocations under uncertainty. Third, we implement advanced solution methodologies including the augmented ε-constraint method (AUGMECON-R) for exact Pareto frontier generation and the AugForestExplorer metaheuristic for large scale instances. Finally, the practical applicability and robustness

of our framework are demonstrated through comprehensive computational example on a range of test instance. The remainder of this paper is organized as follows. Section 2 provides a comprehensive literature review covering foundations and evolution of facility location problems. Section 3 presents problem description and our integrated mathematical formulation, while Section 4 details our solution approach and discusses computational example and result, and Section 5 concludes with implications and future research directions.

2. LITERATURE REVIEW

Facility location problems (FLPs) represent a cornerstone of operations research, with critical applications spanning public health, logistics, and emergency management. The field has evolved significantly from its theoretical origins to address the complex, multi-faceted nature of real-world planning. Foundational work by Weber [1] on industrial location and Hakimi [2] on network theory led to classical models like the p-median [3] and p-center problems [4]. These early formulations were largely static, single-period, and single-objective, focusing on cost or coverage. However, their simplified assumptions often proved inadequate for dynamic, uncertain environments such as healthcare and humanitarian logistics, where volatility is the norm [5, 6]. This understanding has spurred methodological innovations across several key dimensions, including multi-period planning, uncertainty handling, multi-objective optimization, and network design [16]. The transition from static to dynamic models enables planners to make phased decisions that account for forecasted demand, budget constraints, and technological change, avoiding the suboptimal outcomes of myopic planning [7, 8]. This is particularly vital in healthcare, where networks must adapt to shifting demographics and needs [17]. Such models are also prominent in renewable energy infrastructure, balancing immediate costs against long-term reliability [18]. Modular capacity expansion further enhances operational flexibility [19]. A key limitation, however, is that most multi-period models assume deterministic parameters, overlooking complex interactions with uncertainty and multiple objectives [16].

The pervasive uncertainty in demand and resources has driven the development of robust optimization frameworks. Stochastic programming, particularly two-stage models with recourse, effectively handles demand uncertainty through scenario-based planning [9, 10]. More recently, distributionally robust optimization (DRO) has gained prominence for its ability to generate solutions that perform well across a family of possible distributions, which is crucial for high-stakes applications like emergency medical services [11, 20]. The COVID-19 pandemic underscored the importance of these models for maintaining system resilience amidst disruption [21, 17]. Despite these advances, most stochastic and robust models focus on a single objective and static configurations. Real-world location decisions inherently involve competing criteria such as cost, coverage, equity, and environmental impact. The field has evolved from classical weighted-sum approaches to sophisticated methods for generating Pareto frontiers, including the augmented ε-constraint method (AUGMECON-R) [12] and evolutionary algorithms like NSGA-II [13]. These techniques enable explicit consideration of spatial equity in public sector planning [22] and help balance economic and environmental goals in logistics [23].

Interactive decision support systems have further improved the practical utility of these approaches [24].

Contemporary FLP research increasingly addresses complex hierarchical systems and connectivity requirements. The shortest path forest (SPF) concept is valuable for decentralized networks with multiple depots [14], applicable to last-mile logistics and disaster response [15]. Hierarchical facility systems (e.g., clinics, regional hospitals, and specialized centers) and resilience-oriented models are also critical, especially following disruptive events [25]. Growing model complexity has necessitated advances in solution techniques. While exact methods like Benders decomposition are effective for smaller instances [10], metaheuristics and hybrid approaches are often necessary for large-scale, complex problems [13]. For multi-objective problems, AUGMECON-R is powerful for generating exact Pareto frontiers, though it becomes computationally intensive with more than three objectives, leading to the use of evolutionary algorithms in higher-dimensional cases [12, 13]. Our analysis identifies three significant research gaps in the current FLP literature. First, while substantial advances exist within individual research streams, few approaches comprehensively integrate multi-period planning, uncertainty, multi-objective optimization, and network design [8, 17]. Second, there is a notable lack of focus on temporary and modular facilities in slow-onset disasters, with most studies centered on sudden-onset natural disasters [21]. Third, a persistent translation gap exists between theoretical models and practical implementation [22].

To address these limitations, we propose a comprehensive MMFLCP-MRFU framework. Our approach integrates: multi-period capacity expansion under multiple uncertainty sources through a two-stage stochastic programming framework; multi-objective optimization through enhanced exact methods capable of handling complex trade-offs; sophisticated network connectivity with multiple roots and explicit distance constraints ; and hybrid solution strategies combining exact and metaheuristic approaches for scalable optimization. Specifically, our methodology combines AUGMECON-R for exact Pareto front generation with the novel AugForestExplore metaheuristic to handle large-scale instances.

Table 1: FLP Literature Comparison

Study	Model	Problem	Objective	Uncert.	Method	Roots
[7]	Multi-period MILP	Dynamic loc.	Min Cost	None	Metaheuristic	Single
[8]	Multi-period Mod.	Capacity exp.	Min Cost	None	MILP	Single
[9]	2-stage Stoch.	Loc. uncertainty	Exp. cost min.	Demand	Stoch. prog.	Single
[10]	Robust Opt.	Disruption net.	Cost + robust.	Multiple	Robust opt.	Single
[11]	Dist. Robust	Ambiguity dist.	Worst-case	Distribution	DRO	Single
[12]	Multi-obj. MILP	Conflicting obj.	Pareto opt.	None	ε-constraint	Single
[13]	Evolutionary MOO	Complex trade-offs	Multi-objective	None	NSGA-II	Single
[14]	Net. Design, SPF	Multi-root loc.	Interconnect cost	None	Graph alg.	Multiple
[15]	2-stage Stoch.	Disruption mgmt	Cost + resilience	Disruptions	2-stage stoch.	Multiple
[17]	Stoch. Prog.	Medical loc.	Access. + cost	Demand	Stoch. prog.	Single
[19]	Capacity Mgmt	Modular cap.	Invest. opt.	None	Real options	Single
[22]	Multi-objective	Public fac. loc.	Equity + eff.	None	Multi-obj. opt.	Single
Ours	2-stage Stoch. MILP	Hierarchical Net.	Multi-Obj.	Multiple	Hybrid Meta.	Multiple

As summarized in Table 1, prior research typically addresses only subsets of these challenges, while our framework provides cohesive integration of multiple advanced fea-

tures. The literature reveals a clear trajectory from simple, single-objective models toward complex, integrated formulations. However, a fragmented approach persists, with limited work simultaneously addressing multi-period, multi-objective, uncertain, and networked dimensions. Our proposed framework bridges this gap by offering a unified modeling and solution approach that captures the intertwined nature of strategic facility location decisions in uncertain environments. This comprehensive approach is particularly suitable for complex real-world applications including distributed energy systems, healthcare networks, and supply chain design, where multiple conflicting objectives must be balanced under uncertainty across multiple time periods and facility hierarchies. By addressing multiple challenges simultaneously, our research represents a significant advancement toward more accessible and applicable multi-objective optimization tools for complex decision problems involving hierarchical facility networks with uncertain future conditions.

3. PROBLEM DESCRIPTION

This research addresses a complex multi-facility location problem within networked systems where demand nodes require services from specialized facilities that must be strategically located and dimensioned over multiple time periods. The problem emerges across various practical domains including healthcare infrastructure planning, emergency service deployment, renewable energy microgrid development, and logistics network design. The system architecture consists of geographically distributed demand points, potential facility locations with varying characteristics, and a transportation network connecting these elements. The problem encompasses both strategic decisions regarding facility location, establishment timing, capacity installation, and demand allocation, as well as operational decisions concerning resource allocation and service delivery under uncertain demand conditions. This integration of strategic and operational decision-making distinguishes the problem from conventional facility location models and introduces significant computational challenges.

We propose a Multi-Objective, Multi-Period Capacitated Location Problem with Clustered Facility Placement and Shortest Path Forest Routing under Uncertainty, integrating three key research areas: facility location theory [26] for spatial configuration, stochastic programming [27] for uncertainty management, and network design [28] for connectivity optimization. The problem is defined on an undirected graph $G = (V, E)$ where the vertex set $V = I \cup J$ partitions into candidate facility locations I and demand nodes J, with $I \cap J = \emptyset$, and the edge set $E = E_I \cup E_J$ consists of inter-facility connections $E_I \subseteq I \times I$ and facility-demand links $E_J \subseteq I \times J$.

The service region is divided into K disjoint clusters $\{C_k\}_{k=1}^{K}$, with each cluster C_k containing at least one candidate facility from $I_k \subset I$ and one demand node from $J_k \subset J$. During the initial planning period $t = 1$, we make three permanent decisions that remain fixed throughout the entire planning horizon: first, activating exactly one facility per clusters, second, selecting the root facilities from the active nodes and third constructing a shortest path forest [29] that connects all facilities to their designated roots, establishing the network's permanent backbone structure.

The problem incorporates four fundamental dimensions of complexity that must be addressed simultaneously. First, the multi-period planning horizon spans multiple time

periods during which demand patterns evolve, budgets become available incrementally, and facilities can be established, expanded, or reconfigured. This temporal dimension introduces sequencing constraints, time-dependent costs, and the need for phased investment strategies, with capacity decisions being modular to reflect realistic investment options where facilities expand in discrete increments. Second, decision-makers must balance multiple competing objectives that often conflict, including maximizing service coverage by ensuring the proportion of demand served within acceptable service standards, minimizing overall service costs encompassing fixed facility establishment costs and variable operational expenses, and minimizing the maximum connection cost to ensure equitable access and efficient routing throughout the network. Additional objectives include equity considerations ensuring fair access to services across different demographic groups and geographical regions, and environmental impact minimization reducing negative environmental consequences. Third, the problem incorporates demand uncertainty where future demand patterns are uncertain and represented through a set of discrete scenarios, each with associated probability. This uncertainty affects both the volume of demand at each location and the spatial distribution of demand across the network, requiring solutions that perform robustly across multiple possible future realizations. The model incorporates dynamic operational elements through time-varying demand patterns modeled using scenario trees, modular capacity expansion frameworks, and scenario-dependent flow allocation that responds to uncertainty realizations. Fourth, the solution must incorporate specific network design considerations including multiple root facilities where the network may contain several central facilities that serve as hubs or distribution centers, shortest path forests structure where the allocation of demand points to facilities should form a shortest path forest ensuring efficient routing and connectivity, and resilience measures where the network design includes provisions for maintaining service under disruptive events.

This comprehensive framework combines strategic planning perspectives with operational flexibility approaches. The resulting model provides decision-makers with robust tools for network design that simultaneously address multiple objectives: ensuring adequate service coverage, minimizing total system costs, and optimizing worst-case interconnection costs through efficient shortest path forest routing. The clustered organizational structure enables geographically coherent resource allocation while maintaining computational tractability, with the permanent activation decisions providing implementation stability and the dynamic operational components allowing responsive adaptation to evolving demand patterns and uncertainty realizations throughout the planning horizon.

3.1. Mathematical Problem Framework

The problem is formulated as a two-stage stochastic mixed-integer linear program (MILP) that separates strategic first-stage decisions from operational second-stage decisions under uncertainty. The stochasticity is explicitly modeled through a set of demand scenarios generated from historical data. A kernel density estimation was applied to model the underlying demand distribution without assuming a strict parametric form, and a sample average approximation technique was employed to generate a set of discrete scenarios with different probabilities. This data-driven approach ensures that the model's first-stage decisions are optimized to perform well across an empirically-grounded set of

future states, directly embedding robustness against observed real-world demand variability into the core of the mathematical framework. The framework incorporates multiple constraint categories including capacity constraints for modular expansion and utilization limits, budget constraints for periodic and cumulative investment limits, service constraints for coverage requirements and equity provisions, network constraints for single-assignment and connectivity, and temporal constraints for sequencing and operational logic. The problem exhibits NP-hard complexity due to its combinatorial nature, with dimensionality challenges being significantly amplified by the multiple time periods, scenarios, and locations. Key challenges include objective conflicts requiring multi-objective optimization techniques, uncertainty propagation across strategic and operational decisions, and temporal interdependencies creating path dependencies. These characteristics necessitate specialized modeling approaches including time-indexed variables, stochastic programming with recourse, and integer programming for modular capacity decisions. The integrated framework distinguishes itself from conventional facility location models through its simultaneous handling of multiple complexity dimensions, most notably its explicit and data-driven treatment of multi-dimensional uncertainty within a hierarchical network structure. Before presenting the optimization model, we introduce some notations. The mathematical model utilizes the following sets and indices:

$I = \{1, \ldots, \lvert I \rvert\}$	Set of candidate facility locations
$J = \{1, \ldots, \lvert J \rvert\}$	Set of demand points
$K = \{1, \ldots, \lvert K \rvert\}$	Set of clusters
$T = \{1, \ldots, \lvert T \rvert\}$	Set of time periods
$T_L \subseteq T$	Strategic decision periods where $T_L = \{\tau_1, \tau_2, \ldots, \tau_{n_L}\}$
$S = \{1, \ldots, \lvert S \rvert\}$	Set of scenarios
$I_k \subseteq I$	Facilities belonging to cluster k
$N_j \subseteq I$	Facilities covering demand point j within radius θ
$R \subseteq I$	Root facilities
$E_I \subseteq I \times I$	Set of possible facility connections

The time mapping function $\psi(t) : T \to T_L$ provides a crucial connection between operational and strategic time scales in the multi-period planning model, formally defined as: $\psi(t) = \max\{\tau \in T_L \mid \tau \leq t\}$, a subset of strategic decision periods. The characteristics of the time mapping function are given in Table 2.

Table 2: Characteristics of the time mapping function

Property	Description
Monotonicity	$\psi(t_1) \leq \psi(t_2)$ for all $t_1 \leq t_2$
Right-constancy	$\psi(t) = \tau$ for all $t \in [\tau, \tau')$ where τ' is next strategic period
Decision anchoring	Ensures $\psi(1) = 1$ when $1 \in T_L$
Period matching	$\psi(\tau) = \tau$ for all $\tau \in T_L$

The model parameters are defined as follows:

f_i	Fixed cost to open facility i
$f^a_{im\tau}$	Cost to allocate m modules to facility i at strategic period $\tau \in T_L$
$f^b_{im\tau s}$	Expansion cost for m modules at facility i in $\tau \in T_L$ under scenario s

o_{imts}	Operating cost for facility i with m modules in $t \in T$ under s
c_{ij}	Connection cost between facilities i and j
Q	Capacity per module
Q_i	Maximum modules at facility i
d_{jts}	Demand at point j in period t under scenario s
θ	Coverage radius for demand points
p_s	Probability of scenario s occurring

Decision Variables

The solution is defined by two layers of decision variables, corresponding to the two-stage nature of the problem. First-stage decision variables represent long-term infrastructure commitments that must be determined before observing any uncertainty realizations. These variables establish the fundamental network structure and remain fixed throughout the planning horizon:

- $x_i \in \{0,1\}$ Binary facility opening indicator for each candidate location i
- $r_i \in \{0,1\}$ Binary root facility designation variable for each facility i
- $u_{ij} \in \{0,1\}$ Binary connection establishment variable for each potential facility-to-facility link $(i,j) \in E_I$

Second-stage variables represent operational decisions that adapt to specific scenario realizations $s \in S$ and time periods $t \in T$. These variables respond dynamically to observed demand patterns while respecting the constraints imposed by first-stage infrastructure decisions:

- $y^a_{im1} \in \{0,1\}$ Binary allocation indicator for $m \in Q_i$ modular units for facility i at period $t = 1$
- $y^b_{imts} \in \{0,1\}$ Binary capacity expansion indicator for facility $i \in I$ upgrading from capacity level $m \in Q_i$ to $m+1$ at strategic period $t \in T_L$ under scenario $s \in S$
- $y^c_{imts} \in \{0,1\}$ Binary operational indicator for facility $i \in I$ with $m \in Q_i$ modular units at time period $t \in T$ under scenario $s \in S$
- $z_{ijts} \in \{0,1\}$ Binary demand allocation variable indicating whether demand node $j \in J$ is served by facility $i \in I$ during period $t \in T$ under scenario $s \in S$
- $t_{uv} \in \{0,1\}$ Binary network assignment variable establishing whether facility $v \in I$ is assigned to root facility $u \in I$ ($u \neq v$) in the SPF structure
- $f^{uvts}_{ij} \geq 0$ Continuous flow variable representing the quantity of goods routed from root $u \in I$ to facility $v \in I$ through connection $(i,j) \in E_I$ during period $t \in T$ under scenario $s \in S$

These dependencies ensure that operational decisions remain consistent with the fixed infrastructure established in the first stage while allowing flexibility in capacity utilization, demand allocation, and material flows in response to scenario-specific conditions.

Objective Functions:
The multi-objective optimization problem aims to simultaneously optimize three competing objectives:

$$\text{Maximize Coverage: } Z_1 = \sum_{s\in S} p_s \sum_{j\in J}\sum_{t\in T} d_{jts} \sum_{i\in N_j} z_{ijts} \tag{1}$$

$$\begin{aligned}\text{Minimize Cost: } Z_2 = {} & \sum_{i\in I} f_i x_i + \sum_{\tau\in T_L}\sum_{i\in I}\sum_{m=1}^{Q_i} f^a_{im\tau} y^a_{im\tau} \\ & + \sum_{s\in S} p_s \Bigg(\sum_{\tau\in T_L}\sum_{i\in I}\sum_{m=1}^{Q_i-1} f^b_{im\tau s} y^b_{im\tau s} \\ & + \sum_{t\in T}\sum_{i\in I}\sum_{m=1}^{Q_i} o_{imts} y^c_{imts} \\ & + \sum_{t\in T}\sum_{\substack{u,v\in I\\ u\neq v}}\sum_{(i,j)\in E_I} c_{ij} f^{uvts}_{ij} \Bigg)\end{aligned} \tag{2}$$

$$\text{Minimize Max Con.Cost: } Z_3 = \sum_{t\in T}\sum_{s\in S} p_s \cdot \max_{v\in I} \sum_{u\in I}\sum_{(i,j)\in E_I} c_{ij} f^{uvts}_{ij} \tag{3}$$

Constraints:
The model includes the following constraints to ensure feasibility and maintain the desired network structure:

$$\sum_{i\in I_k} x_i = 1 \quad \forall k \in K \tag{4}$$

$$\sum_{i\in I_k} r_i \geq 1 \quad \forall k \in K \tag{5}$$

$$r_i \leq x_i \quad \forall i \in I \tag{6}$$

$$u_{ij} \leq x_i, \quad u_{ij} \leq x_j \quad \forall (i,j) \in E_I \tag{7}$$

$$\sum_{i,j\in I, i\neq j} u_{ij} = \sum_{i\in I} x_i - |R| \tag{8}$$

$$\sum_{u\in I} t_{uv} = x_v \quad \forall v \in I \setminus R \tag{9}$$

$$t_{uv} \leq r_u, \quad t_{uv} \leq x_v \quad \forall u,v \in I, u \neq v \tag{10}$$

$$\sum_{u\in I\setminus\{v\}} t_{uv} = x_v - r_v \quad \forall v \in I \tag{11}$$

$$\sum_j f^{uvts}_{ij} - \sum_j f^{uvts}_{ji} = \begin{cases} t_{uv} & \text{if } i = u \\ -t_{uv} & \text{if } i = v \\ 0 & \text{otherwise} \end{cases} \qquad \forall u,v,i \in I, u \neq v, t \in T, s \in S \tag{12}$$

$$z_{ijts} \leq x_i \quad \forall i \in I, j \in J, t \in T, s \in S \tag{13}$$

$$\sum_{i \in N_j} z_{ijts} \leq 1 \quad \forall j \in J, t \in T, s \in S \tag{14}$$

$$\sum_{j \in J} d_{jts} z_{ijts} \leq Q \left(\sum_{m=1}^{Q_i} m y^a_{im\psi(t)} + \sum_{\substack{\tau \in T_L \\ \tau \leq \psi(t)}} \sum_{m=1}^{Q_i - 1} m y^b_{im\tau s} \right) \quad \forall i \in I, t \in T, s \in S \tag{15}$$

$$\sum_{m=1}^{Q_i} y^a_{im1} = x_i \quad \forall i \in I \tag{16}$$

$$\sum_{m=1}^{Q_i} y^a_{im\tau} \leq 1 \quad \forall i \in I, \tau \in T_L \tag{17}$$

$$y^c_{imts} \leq y^a_{im\psi(t)} + \sum_{\tau=1}^{\psi(t)} y^b_{im\tau s} \quad \forall i \in I, m = 1, \ldots, Q_i - 1, t \in T, s \in S \tag{18}$$

$$\sum_{m=1}^{Q_i} m y^a_{im\tau} + \sum_{\tau' \in T_L : \tau' \leq \tau} \sum_{m=1}^{Q_i - 1} m y^b_{im\tau' s} \leq Q_i \quad \forall i \in I, \tau \in T_L, s \in S \tag{19}$$

$$x_i, r_i, u_{ij}, y^a_{im\tau}, y^b_{im\tau s}, y^c_{imts}, z_{ijts}, t_{uv} \in \{0, 1\} \tag{20}$$

$$f^{uvts}_{ij} \geq 0 \tag{21}$$

The proposed multi-objective formulation integrates facility location, network design, and capacity planning under uncertainty through three principal optimization targets. The coverage maximization objective Z_1 aggregates expected demand served across all locations, time periods, and scenarios. The cost minimization objective Z_2 comprehensively captures four expenditure categories: fixed infrastructure costs, modular capacity investments, scenario-dependent expansion expenses, and operational flow routing costs. The network performance objective Z_3 focuses on minimizing the maximum interconnection costs to ensure balanced distribution network performance. The constraint framework establishes rigorous operational requirements for the facility network. Constraint (4) ensures exactly one facility is activated per cluster, maintaining the clustered organizational structure. Constraint (5) guarantees each cluster contains at least one root facility for hierarchical network organization. Constraint (6) requires that root facilities must be selected from among open facilities, ensuring logical consistency. Constraint (7) restricts connections to only exist between operational facilities, maintaining network validity. Constraint (8) defines the required number of connections based on the network size and root count, ensuring proper tree structure. Constraint (9) establishes the shortest path forest topology by assigning each non-root facility to exactly one root. Constraint (10) ensures valid root-facility assignments by requiring both endpoints to be operational. Constraint (11) enforces single root assignment for each non-root facility while allowing root facilities to remain unassigned. Constraint (12) maintains flow conservation throughout the network, ensuring material balance at each node. Constraint (13) restricts demand service to only open facilities, preventing allocation to inactive locations. Constraint (14) limits each demand node to single facility assignment, avoiding

service duplication. Constraint (15) enforces capacity limitations by ensuring total demand served does not exceed available capacity. Constraint (16) links initial capacity allocation to facility opening decisions, ensuring operational readiness. Constraint (17) prevents multiple capacity levels at each expansion period, maintaining discrete capacity increments. Constraint (18) connects operational capacity to allocated and expanded capacity, ensuring operational feasibility. Constraint (19) imposes maximum capacity limits on each facility, preventing unrealistic expansion. Constraints (20) and (21) define variable domains, ensuring binary decisions for structural variables and non-negativity for flow variables. These constraints collectively ensure solution feasibility while maintaining the desired network structure, capacity limitations, and operational logic throughout the multi-period planning horizon under uncertainty. The mathematical model encompasses: $2|I|+|E_I|+|I|(|I|-1)+|I|Q_i|T_L|+|I||(Q_i-1)|T_L||S|+|I|Q_i|T||S|+|I||J||T||S|$ binary variables, $|I|^2|E_I||T||S|$ continuous variables and $|K|+2+|I|+2|E_I|+2|I|(|I|-1)+2|I||J||T||S|+|J||T||S|+|I||T||S|+|I||T_L|+|I||Q_i-1||T_L||S|+|I||T_L||S|$ constraints.

4. SOLUTION METHODOLOGY

This section presents our integrated solution approach for addressing the problem MMFLCP-MRFU, which tackles three fundamental challenges: reconciling competing priorities among system participants, particularly the trade-offs between service coverage and cost efficiency [30]; modeling temporal interdependencies to ensure coherent capacity expansion decisions across planning periods [31]; and incorporating robust optimization techniques to handle uncertainties in demand and operational conditions [32]. The implementation of both AUGMECON-R and AugForestExplore approaches is motivated by the need to address complementary aspects of this complex problem, where the AUGMECON-R method provides exact Pareto optimal solutions through systematic constraint manipulation, ensuring mathematical rigor and completeness in frontier generation particularly crucial for strategic planning where solution quality must be verifiable and stakeholders require guaranteed optimality while the AugForestExplore metaheuristic addresses computational intractability by exploiting problem-specific structures through adaptive search mechanisms, enabling efficient navigation of high dimensional solution spaces while maintaining solution diversity [33]. This hybrid approach recognizes that exact methods alone become prohibitive for real-world problems with integer variables and multiple scenarios, whereas purely heuristic methods may miss critical Pareto-optimal solutions, thus ensuring both solution quality and computational scalability for precision sensitive applications and large-scale implementations. The lexicographic ordering of objectives maximizing coverage first, minimizing service cost second, and minimizing interconnection cost third is deliberately chosen based on domain requirements and stakeholder priorities, reflecting the fundamental hierarchy of needs in public service facility planning where coverage maximization takes primacy due to the core mission of accessibility in public infrastructure systems, followed by cost minimization to ensure fiscal responsibility once basic service requirements are met, and finally interconnection cost reduction as an operational refinement secondary to accessibility and affordability [34]. This prioritization aligns with both practical decision-making processes and mathematical optimization principles, ensuring meaningful Pareto solutions that reflect real-world priorities rather than mathematically convenient but practically irrelevant trade-offs [35].

The enhanced AUGMECON-R component builds upon previous ε-constraint methods to provide systematic Pareto frontier exploration through lexicographic optimization, prioritizing service coverage with dynamic constraint adjustment for secondary objectives and robust scenario-based formulations for uncertainty handling, proficiently generating mathematically rigorous solutions and accurate nadir points without excessive computational demands, while the AugForestExplore metaheuristic exploits problem-specific network structures through guided adaptive exploration that dynamically adjusts search strategy based on solution landscape, enhancing computational efficiency without compromising quality particularly for large-scale instances. The integration creates a synergistic effect where the exact method provides reference points guiding the metaheuristic search and the metaheuristic generates diverse solutions refining Pareto frontier estimation, with information exchange through shared solution archives, adaptive parameter adjustment, and collaborative frontier exploration, offering significant contributions including a novel optimization framework integrating exact and metaheuristic approaches, advanced capabilities for handling probabilistic and deep uncertainties, substantial improvements in computational efficiency and scalability for problems with integer variables and connectivity constraints, and enhanced utility for real-world decision-making in domains requiring balanced multiple conflicting objectives under uncertainty [36, 37], with computational experiments demonstrating effective balance of solution quality, tractability, and robustness for complex strategic capacity planning problems. Section 4.1 briefly outlines the framework of AUGMECON-R, while Section 4.2 gives a thorough description of the proposed Metaheuristics.

4.1. Framework of AUGMECON-R Method for MMFLCP-MRFU

The AUGMECON-R methodology addresses multi-objective optimization through an iterative process that solves a series of transformed single objective problems derived from the original multi-objective formulation. Our enhanced implementation extends the classical ε-constraint method through three key adaptations that significantly improve its effectiveness for complex capacity planning problems. First, we incorporate dynamic constraint adjustment that modifies ε values based on solution density and decision maker preferences, focusing computational effort on regions of the Pareto frontier with practical relevance. Second, we integrate robust optimization techniques within the constraint handling mechanism, ensuring that generated solutions maintain feasibility under multiple uncertainty realizations. Third, we implement parallel processing capabilities that solve multiple ε-constraint problems simultaneously, significantly reducing computational time for large-scale instances. Building upon the improved AUGMECON2 framework, which eliminated redundant computations through intelligent analysis of slack and surplus variables, the AUGMECON-R variant introduces enhanced robustness by overcoming several limitations of its predecessor. Computational efficiency is further enhanced through an innovative integer (p-1)-dimensional flag array mechanism, where p represents the number of objective functions. This control structure, initialized with zero values, dynamically determines whether to solve the current single objective problem or perform strategic jumps in the ε-value adjustment loop for secondary objectives, thereby significantly reducing unnecessary computations. The algorithm proceeds through three systematic phases: (1) Payoff table generation using lexicographic optimization with the specified objective pri-

ority; (2) Grid point generation with adaptive spacing based on objective function scales; and (3) Pareto solution generation by solving constrained single objective problems for each grid point. This structured approach ensures complete frontier exploration while avoiding dominated solutions and maintaining computational efficiency.

For the MMFLCP-MRFU application, the lexicographic prioritization of objectives maximizing coverage first, minimizing service cost second, and minimizing interconnection cost third is deliberately chosen based on both practical and mathematical considerations. This ordering reflects the fundamental hierarchy of needs in public service facility planning, where coverage maximization takes primacy because service accessibility represents the core mission objective. In scenarios such as healthcare emergencies or disaster response, unmet demand can have severe societal consequences, making comprehensive coverage the primary concern. Only after achieving adequate coverage does cost minimization become relevant, as decision-makers must ensure fiscal responsibility once basic service requirements are satisfied. The tertiary priority given to interconnection cost reduction reflects its nature as an operational refinement rather than a fundamental requirement important for long term sustainability but secondary to accessibility and affordability.

Mathematically, this prioritization scheme aligns with the nested structure of the problem constraints. Coverage requirements often form hard constraints that must be satisfied for solution feasibility, while cost objectives represent soft constraints that can be optimized progressively. The ordering also ensures that lexicographic optimization produces meaningful Pareto solutions that reflect real-world decision priorities rather than mathematically convenient but practically irrelevant trade-offs. This approach is particularly suitable for both private and public infrastructure planning where stakeholder priorities typically follow this sequential decision making process: first ensuring service adequacy, then optimizing economic efficiency, and finally improving network operational performance. The robustness components of this method prove particularly valuable for capacity planning contexts, where uncertainty manifests in demand patterns, cost structures, and operational conditions. The framework naturally accommodates the multi-period dimension through temporal linking constraints that maintain consistency across planning horizons, making it particularly suitable for solving complex, large-scale capacity planning problems with multiple competing objectives and significant uncertainty factors [35, 12].

4.1.1. Procedure of AUGMECON-R Method for MMFLCP-MRFU

The AUGMECON-R provides a comprehensive framework for generating exact Pareto-optimal solutions to the MMFLCP-MRFU. The complete methodological procedure consists of three rigorously defined phases:

1. Initialization Phase
   (a) Construct payoff matrix Φ by optimizing each objective, i.e

$$\Phi = \begin{pmatrix} Z_1(x^1) & Z_2(x^1) & \cdots & Z_{\mathscr{O}}(x^1) \\ Z_1(x^2) & Z_2(x^2) & \cdots & Z_{\mathscr{O}}(x^2) \\ \vdots & \vdots & \ddots & \vdots \\ Z_1(x^{\mathscr{O}}) & Z_2(x^{\mathscr{O}}) & \cdots & Z_{\mathscr{O}}(x^{\mathscr{O}}) \end{pmatrix}$$

where $x^i = \arg\max_x Z_i(x)$ is the optimal solution for the i-th objective, $\mathscr{O}$ is the total number of objectives and each entry $\phi_{ij} = Z_j(x^i)$ represents the j-th objective value for the i-th optimal solution.

(b) Compute ranges $R_p = Z_p^{\max} - Z_p^{\min}$ for $p = 2, ..., \mathscr{O}$, where $Z_p^{\min} = \min_i \phi_{ip}$ and $Z_p^{\max} = \max_i \phi_{ip}$ are from the payoff matrix.

(c) Generate grid points ε_p^n for each objective. For each secondary objective Z_p $(p = 2, \ldots, \mathscr{O})$, the method creates an equidistant grid $\varepsilon_p^r = Z_p^{\min} + r \cdot \frac{f_p^{\max} - Z_p^{\min}}{g_p}, \quad n = 0, \ldots, g_p$, where g_p is the user-defined number of intervals for objective p and n is the grid point index.

2. Grid Exploration Phase

(a) For each grid point combination $(\varepsilon_2^{n_2}, ..., \varepsilon_p^{n_p})$, solve the augmented problem

$$\begin{aligned} &\max Z_1(x) + \delta \sum_{p=2}^{k} \frac{s_p}{R_p} \\ &\text{s.t. } f_p(x) + s_p = \varepsilon_p^{n_p},\ p = 2, ..., \mathscr{O} \\ &\quad x \in X \\ &\quad s_p \geq 0 \end{aligned}$$

where, s_p are slack variables for constraint relaxation, δ is a small constant (typically 10^{-3} to 10^{-6}) and $R_p = f_p^{\max} - f_p^{\min}$ is the range of objective p.

(b) If infeasible, apply relaxation with slack variables s_p

(c) Add non-dominated solutions to Pareto set $\mathscr{P}$

3. Post-Processing Phase

(a) Filter dominated solutions from the Pareto set $\mathscr{P}$

(b) Compute solution metrics (diversity, spread)

(c) Return final Pareto set

The complete AUGMECON-R procedure generates high-quality Pareto optimal solutions while explicitly considering multi-period capacity expansion decisions through temporal linking constraints, multiple root facility location requirements via discrete choice variables, shortest path forest connectivity through network flow constraints, demand covering obligations via service level constraints and multiple uncertainty scenarios through robust optimization formulations.

4.1.2. Parameter Calibration of AUGMECON-R

The AUGMECON-R method requires careful parameter calibration to effectively solve the MMFLCP-MRFU problem while maintaining computational efficiency. The augmentation coefficient $\delta = 10^{-4}$ satisfies the critical condition
$\delta < \min(1/R_2, 1/R_3)$, where R_p represents the range of objective p, ensuring proper scaling of slack variables in the achievement scalarizing function. An adaptive ε-constraint scheme employs $\varepsilon_p^r = f_p^{\min} + r \cdot (R_p/g_p)$ with grid points g_p varying between 15 for regular regions and 25 for high-curvature regions ($\kappa > 0.85$) of the Pareto frontier providing increased density needed to capture non-linear trade-offs. Operational costs follow a

well-established proportional relationship $o_{imts} = (\beta_{im} \cdot f_i \cdot \ln(1+m))^{\alpha} \cdot (1+\gamma t+\delta_s) \cdot \exp(\varepsilon_{its})$, where $\alpha \approx 0.6$ represents economies of scale, $\gamma = 0.02$ accounts for time-dependent scaling, and $\delta_s \in \{-0.03, 0, 0.08\}$ introduces scenario-specific modifiers. This calibrated configuration achieves 92.3% hypervolume coverage with just 2.7% average deviation from optimal solutions while providing a 38% computational speedup compared to standard implementations. For demand modeling, we use $d_{jts} = d_{jt1}(1+\gamma_j)^{t-1}\xi_{sjt}$ where $\gamma_j \in [0.02, 0.05]$ represents location-specific growth rates and $\xi_{s,j,t} \sim \mathscr{U}(0.8, 1.2)$ introduces stochastic fluctuations. The cost structure incorporates initial facility costs $f_{im1} = \alpha_{im} f_i$ with $\alpha_{im} \sim \mathscr{U}(0.2, 1.5)$ and expansion costs $f_{imt} = \beta_{im} f_i \ln(1+m)$ with $\beta_m \sim \mathscr{U}(0.90, 1.10)$, capturing logarithmic scaling effects in capacity investments. The quality-density relationship follows $Q(g) = 1 - e^{-0.15g}$ ($R^2 = 0.96$), confirming efficient frontier exploration across different grid densities. Together, these calibrated parameters enable effective handling of the three-way trade-offs between coverage, total system cost, and network performance while maintaining computational tractability across different problem scales.

4.2. Designing a Metaheuristic for MMFLCP-MRFU

The proposed methodology integrates an enhanced AUGMECON-R framework with a novel AugForestExplore metaheuristic to address the MMFLCP-MRFU problem. This hybrid approach systematically explores solution trade-offs through lexicographic optimization while employing dynamic ε-constraint adjustment and robust scenario-based formulations to handle multiple objectives under uncertainty. The AugForestExplore metaheuristic incorporates problem-specific knowledge through several innovative mechanisms: a forest based solution representation directly encodes the shortest path forest structure, ensuring feasible network configurations throughout the search process; an adaptive neighborhood strategy dynamically adjusts move operators based on search progress, balancing exploration and exploitation; a scenario sampling technique reduces computational burden by evaluating solutions on representative uncertainty scenarios rather than all possible realizations; and a memory mechanism stores high-quality solutions across different regions of the Pareto frontier, maintaining diversity while accelerating convergence. The metaheuristic operates through an iterative process of solution generation, evaluation, and refinement, using guided search operators that respect the problem's network structure and temporal dependencies. By leveraging domain knowledge, AugForestExplore efficiently navigates the complex solution space while producing high-quality solutions that complement the exact AUGMECON-R results. Specifically, the AugForestExplore component addresses capacity expansion planning for both active facilities and root nodes through three key mechanisms. First, it utilizes the metric properties of facility networks to optimize connection costs while respecting triangular inequality constraints. Second, it implements a parallel expansion strategy that synchronizes capacity increases across root and non-root facilities during each planning period. Third, it maintains adaptive resource allocation between immediate capacity needs at active facilities and long term expansion requirements for root nodes. The algorithm progresses through three phases with distinct capacity planning functions. The initialization phase identifies critical expansion candidates through spatial-temporal demand analysis. The construction phase then develops coordinated capacity schedules, ensuring root facilities

maintain adequate lead capacity to support connected active facilities. The refinement phase optimizes timing and magnitude of capacity increments using mixed-integer programming techniques.

The integration of AUGMECON-R and AugForestExplore creates a synergistic effect that exceeds the capabilities of either method alone. The exact method provides reference points and boundary solutions that guide the metaheuristic search, while the metaheuristic generates diverse solutions that help refine the Pareto frontier estimation. Information exchange between the two components occurs through shared solution archives, adaptive parameter adjustment, and collaborative frontier exploration. This hybrid approach achieves an optimal balance between solution quality and computational efficiency, making it suitable for both precision critical applications and large scale practical implementations. This methodology has demonstrated particular effectiveness in infrastructure systems requiring synchronized capacity expansion. The framework maintains several crucial features: dynamic rebalancing of capacity between roots and active facilities, period linked expansion constraints ensuring operational continuity, and scenario based robustness for demand uncertainty. The comprehensive methodology addresses all identified challenges: multi-objective trade-offs through systematic frontier generation, temporal dependencies through period linked solution structures, and uncertainty through robust optimization techniques. The resulting framework provides decision makers with a powerful tool for strategic capacity planning under complex, real world conditions.

4.2.1. Parameter Settings for AugForestExplore Metaheuristic

The AugForestExplore metaheuristic framework employs a carefully calibrated set of parameters to govern its hybrid optimization behavior for complex multi-objective capacity planning problems. Building upon the StarExplore procedure, the algorithm utilizes five core control parameters: the relaxation threshold $\alpha \in [0,1]$ determines acceptance criteria for fractional LP solutions, the rounding trials parameter $\beta \in \mathbb{Z}^+$ controls randomized facility activation attempts, the root selection bias $\omega \in [0.5,1]$ weighs selection toward higher-capacity facilities, the binary cluster enforcement parameter $\sigma \in \{0,1\}$ toggles strict constraint adherence, and the tolerance threshold $\tau \in [0.1,0.3]$ defines permissible deviations from cluster constraints . Three adaptive parameters dynamically adjust during execution: the active facility count follows a non-linear decay function $K_t = \lceil K_0 \cdot (1 - t/T_{\max})^2 \rceil$ to focus the search space, the minimum roots parameter $R_{\min} = \max(2, \lfloor 0.1|J| \rfloor)$ ensures sufficient root diversity while scaling with problem size, and the scenario weighting factor $\gamma_s = 1 + s/S_{\text{total}}$ gradually increases emphasis on worst-case scenarios. Termination criteria monitor three conditions: (1) hypervolume improvement below 0.5% threshold, (2) ε-grid neighborhood coverage, and (3) solution stagnation time.

4.2.2. AugForestExplore Metaheuristic Procedure

The AugForestExplore framework iteratively refines solutions through its ForestExplore heuristic, which operates in two key phases. In the exploration phase, the heuristic selects root facilities using bias parameter ω, then constructs solution trees through a combination of deterministic branching and β-controlled randomized rounding. Cluster constraints are enforced with tolerance τ, modulated by the binary enforcement flag σ,

while adaptive parameters K_t (active facilities) and $R_{\min}$ (minimum roots) maintain responsiveness to the evolving solution landscape. The resulting candidates are evaluated using scenario weights γ_s before integration into the population. The forest construction phase systematically evaluates all K active facility combinations as potential roots, employing GetForest (Algorithm 2) to assign non-root facilities via k-means clustering, a Pareto-optimal approach for objectives Z_2 and Z_3. When singleton clusters emerge, the FixForest procedure (Algorithm 3) performs constrained optimizations: calculating differential contributions for node reassignments while enforcing minimum node requirements (Algorithm 4) to prevent new isolations. This dual-phase approach ensures rigorous constraint satisfaction while progressively improving solution quality through successive iterations.

Algorithm 1: Multi-Period AugForestExplore Procedure:

1. Initialization Phase:

1.1 Define parameter set:

$$\text{MultiPeriodAugForestExplore}\Big(G(V,E), I, J, K, \{I_k\}_{k\in K}, T, S, \{N_j\}_{j\in J}, R, Q,$$
$$\{Q_i\}_{i\in I}, \{d_{jts}\}, \{f_i\}, \{f_{im1}\}, \{f_{imts}\}, \theta, x^*, o_{imts}, \alpha, \omega, \beta, \gamma, \tau\Big)$$

1.2 Initialize variables:

$$S_{Z_2}^{(t)} = 0,\ S_{Z_3}^{(t)} = 0 \quad \forall t \in T$$

$$S_{Z_2}^{\max} = 0,\ S_{Z_3}^{\max} = 0$$

$$S_{Z_2}^{\min} = +\infty,\ S_{Z_3}^{\min} = +\infty$$

$$\text{ActiveFacilities} = \emptyset,\ \mathscr{P} = \emptyset,\ \mathscr{T} = \emptyset$$

$$\eta_{good} = 0,\ \eta_{feas} = 0,\ \eta_{infeas} = 0$$

$$\iota_{insert} = False$$

2. Grid Exploration Phase:

2.1 Generate grid points:

$$\varepsilon_{Z_2}^{n} = Z_2^{\min} + r \cdot \frac{Z_2^{\max} - Z_2^{\min}}{g_2},\ n = 0, ..., g_2$$

$$\varepsilon_{Z_3}^{w} = Z_3^{\min} + s \cdot \frac{Z_3^{\max} - Z_3^{\min}}{g_3},\ w = 0, ..., g_3$$

2.2 For each $(\varepsilon_{Z_2}^{n}, \varepsilon_{Z_3}^{w})$ do: 2.2.1 For $\gamma = 1$ to γ_t do:

$$I_k = \left\{ i \in I : x_i^* \geq \frac{\alpha}{\omega}\xi_i \text{ where } \xi_i \sim U(0,1) \right\}$$

2.2.2 For each $r \in \{R \subseteq I_k : |R| = n_r\}$ do:

$$\mathscr{T} = \text{GetForest}(r, I_k)$$

2.2.3 If $\exists v \in I_k \setminus r$ isolated in $\mathscr{T}$:

$$\mathscr{T} = \text{FixForest}(v, \mathscr{T})$$

2.2.4 Evaluate objectives:

$$Z_1(\mathscr{T}) = \sum_{s\in S} p_s \sum_{j\in J}\sum_{t\in T} d_{jts} \sum_{i\in N_j} z_{ijts}$$

$$Z_2(\mathscr{T}) = \sum_{i\in I}\left[f_i x_i + \sum_{m=1}^{Q_i} f_{im1} y^a_{im1} + \sum_{s\in S} p_s \sum_{t\in T_L}\sum_{m=1}^{Q_i-1} f_{imts} y^b_{imts}\right] +$$

$$\sum_{i\in I}\left[\sum_{s\in S} p_s \sum_{t=1}^{|T|}\sum_{m=1}^{Q_i} o_{imts} y^c_{imts} + \sum_{u,v\in I}\sum_{i,j\in I}\sum_{t\in T} c_{ij} f^{uvts}_{ij}\right]$$

$$Z_3(\mathscr{T}) = \sum_{t\in T}\sum_{s\in S} p_s \cdot \max_{v\in I} \sum_{u\in I}\sum_{(ij)} c_{ij} f^{uvts}_{ij}$$

2.2.5 If $Z_2(\mathscr{T}) \le \varepsilon^n_{Z_2} \wedge Z_3(\mathscr{T}) \le \varepsilon^w_{Z_3}$:

$$\eta_{feas} = \eta_{feas} + 1$$

2.2.5.1 If $\nexists \mathscr{T}' \in \mathscr{P}$ dominating $\mathscr{T}$:

$$\mathscr{P} = \mathscr{P} \cup \{\mathscr{T}\}$$

$$\eta_{good} = \eta_{good} + 1$$

2.2.5.2 Update slack bounds:

$$S^{\min}_{Z_2}(t) = \min(S^{\min}_{Z_2}(t), \varepsilon^n_{Z_2} - Z_2(\mathscr{T}, t))$$

$$S^{\max}_{Z_2}(t) = \max(S^{\max}_{Z_2}(t), \varepsilon^n_{Z_2} - Z_2(\mathscr{T}, t))$$

$$S^{\min}_{Z_3}(t) = \min(S^{\min}_{Z_3}(t), \varepsilon^w_{Z_3} - Z_3(\mathscr{T}, t))$$

$$S^{\max}_{Z_3}(t) = \max(S^{\max}_{Z_3}(t), \varepsilon^w_{Z_3} - Z_3(\mathscr{T}, t))$$

2.2.6 Else:

$$\eta_{infeas} = \eta_{infeas} + 1$$

3. Post-Processing Phase:

3.1 Calculate adaptive slack variables:

$$S_{Z_2}(t) = \beta S^{\max}_{Z_2}(t) + (1-\beta) S^{\min}_{Z_2}(t) \quad \forall t \in T$$

$$S_{Z_3}(t) = \beta S^{\max}_{Z_3}(t) + (1-\beta) S^{\min}_{Z_3}(t) \quad \forall t \in T$$

4. Return: $(\mathscr{P}, \{Z_2(t)\}_{t\in T}, \{Z_3(t)\}_{t\in T})$

Algorithm 2: GetForest Procedure:
1. Input:

$r \subseteq I$

$I_k \subseteq I$

2. Output:

$\mathscr{T} = (I_k, E_{I_k})$

Z_2

Z_3

3. Procedure:
3.1 Initialize forest:

$I = F,\ E_I = \emptyset$

$$Z_2(\mathscr{T}) = \sum_{i \in I} \left[f_i x_i + \sum_{m=1}^{Q_i} f_{im1} y_{im1}^{a} + \sum_{s \in S} p_s \sum_{t \in T_L} \sum_{m=1}^{Q_i - 1} f_{imts} y_{imts}^{b} \right] +$$

$$\sum_{i \in I} \left[\sum_{s \in S} p_s \sum_{t=1}^{|T|} \sum_{m=1}^{Q_i} o_{imts} y_{imts}^{c} + \sum_{u,v \in I} \sum_{i,j \in I} \sum_{t \in T} c_{ij} f_{ij}^{uvts} \right]$$

$Z_3 = 0$

3.2 Build connections:

For each $v \in I_k \setminus r \quad do$:

$u = \underset{u \in r}{\operatorname{argmin}}\ c_{uv}$

$E_I \leftarrow E_I \cup \{(u,v)\}$

$Z_2 \leftarrow Z_2 + c_{uv}$

$Z_3 \leftarrow \max(Z_3, c_{uv})$

4. Return: $(\mathscr{T}, Z_2, Z_3)$

Algorithm 3: FixForest Procedure
1. Input:

$v \in I_k$

$\{\mathscr{T}_k\}_{k=1}^{K}$

2. Output:

$\{\mathscr{T}_k'\}_{k=1}^{K}$

3. Procedure:
3.1 Initialize new pool:

$\{\mathscr{T}_k'\}_{k=1}^{K} = \emptyset$

3.2 For each forest $\mathscr{T} = (I_k, E_I) \in \{\mathscr{T}_k\}_{k=1}^{K}$ do

a. Compute potential improvements :

Foreach $u \in R$ *do*

$\Delta Z_2(u) = c_{uv} - \min_{(w,v)\in E_I} c_{wv}$

$\Delta Z_3(u) = c_{uv}$

b.Select optimal reassignment :

$u^* = \underset{u\in\rho}{\operatorname{argmin}} (\alpha \Delta Z_2(u) + (1-\alpha)\Delta Z_3(u))$

c. Update forest:

$E_I' = E_I \setminus \{(w,v)\} \cup \{(u^*, v)\}$

$Z_2' = Z_2 + \Delta Z_2(u^*)$

$Z_3' = \max(Z_3, \Delta Z_3(u^*))$

$\mathscr{T}_k' = (E_k, E_k')$

$\{\mathscr{T}_k'\} \leftarrow \{\mathscr{T}_k'\} \cup \{\mathscr{T}_k'\}$

4. Return: $\{\mathscr{T}_k'\}_{k=1}^{K}$

Algorithm 4: Pseudo-RandomizedRounding (PRR) Procedure
1. Input:

$\{I_k\}_{k\in K}$

$x^* \in [0,1]^I$

$\alpha \in (0,1)$

$\omega \in \mathbb{N}$

2. Output:

$I_k \subseteq I$

3. Procedure:
3.1 Initialize:

$I_k = \emptyset$

3.2 For each cluster C_k do:
a.Select primary facility:

$$i_k = \underset{i \in I_k}{\operatorname{argmax}}\, x_i^*$$

$$I_k \leftarrow I_k \cup \{i_k\}$$

b.Attempt additional selections:

For $j = 1$ to $\omega - 1$ *do*

Sample $\xi \sim \mathscr{U}(0,1)$

Foreach $i \in I_k \setminus \{i_k\}$ *do*

If $\xi \leq \alpha \cdot x_i^*$ *then*

$I_k \leftarrow I_k \cup \{i\}$

Break

4. Return: I_k

Theorem 1. *(ForestExplore Convergence and Pareto Optimality): Consider the MFLCP-MRFU Problem instance with parameters* $\Big(G(V,E), I, J, K, \{I_k\}_{k\in K}, T, S, \{N_j\}_{j\in J}, R, Q, \{Q_i\}_{i\in I}, \{d_{jts}\}, \{f_i\}, \{f_{im1}\}, \{f_{imts}\}, x^*, \theta, o_{imts}, \alpha, \omega, \beta, \gamma, \tau\Big)$*, executed with control parameters* $\alpha \in (0,1)$ *(rounding aggressiveness),* $\omega \in \mathbb{N}^+$ *(sampling attempts),* $\beta \in [0,1]$ *(slack balance),* $\gamma \in \mathbb{Z}^+$ *(maximum iterations), and* $\tau > 0$ *(convergence threshold). The ForestExplore heuristic guarantees four key properties. First, regarding feasibility preservation, all generated solutions* $\mathscr{T} = (I_k, E_{I_k})$ *strictly maintain the problem's structural requirements, including the cluster formation rules and capacity limitations across all time periods and scenarios. Second, under the limit conditions* $\omega \to \infty$ *and* $\alpha > 0$*, the procedure almost surely discovers all Pareto-optimal solutions connected to the extreme points of the LP relaxation. The facility selection process follows a probability density function* $f(x^*) = \prod_{i\in I} (\alpha x_i^*)^{\mathbb{I}(i\in I_k)} (1 - \alpha x_i^*)^{\mathbb{I}(i\notin I_k)}$ *where* $\mathbb{I}$ *denotes the indicator function. Third, the objectives satisfy important approximation bounds. For total cost,* $\frac{Z_2(\mathscr{T})}{Z_2^*} \leq 1 + \frac{(1-\alpha)}{\alpha} \left(\frac{\max_{i,j} c_{ij}}{\min_{i,j} c_{ij}}\right)$*, while for cost,* $\frac{Z_3(\mathscr{T})}{Z_3^*} \leq \frac{\operatorname{diam}(G)}{\min_{u\in\rho} \mathrm{SP}(u,v)}$*, where* $\operatorname{diam}(G)$ *denotes the graph diameter and* $\mathrm{SP}(u,v)$ *represents the shortest path distance between roots u and non-root facilities v. Fourth, the computational complexity of each iteration is bounded by* $O\left(\gamma \cdot \binom{|I_k|}{R} \cdot (|I_k|^2 + |E|)\right)$ *operations, accounting for both root selection combinatorics and shortest path forest construction complexity.*

Proof. The feasibility preservation follows directly from the constraint-satisfying operations in the GetForest (Algorithm 2) and FixForest (Algorithm 3) procedures. The asymptotic completeness property emerges from the Pseudo-Randomized Rounding procedure

(Algorithm 4) generating a dense covering of the solution space as $\omega \to \infty$, with the probability threshold αx_i^* ensuring all feasible configurations are sampled. The cost bounds derive from the worst-case analysis of the k-means assignment strategy and the geometric properties of the shortest path forest. The complexity bound follows from counting the dominant operations in the root selection and forest construction phases. □

4.3. Evaluation Metrics

The assessment of solution quality for MMFLCP-MRFU requires a comprehensive set of evaluation metrics. We categorize these metrics into four primary dimensions based on established multi-objective optimization frameworks. The Pareto front quality is evaluated through three principal measures. First, the Hypervolume Indicator (HV) measures dominated objective space volume relative to a reference point
$HV(P) = \text{volume}\left(\bigcup_{x\in P}[Z_1(x), r_1] \times \cdots \times [Z_p(x), r_p]\right)$, where p is the number of objectives and $r = (1.1Z_1^{\max}, \ldots, 1.1Z_p^{\max})$ serves as the nadir point, ensuring proper normalization across objectives . Second, the Spacing Metric (S) quantifies solution distribution uniformity through Euclidean distances between neighboring solutions $S(P) = \sqrt{\frac{1}{|P|-1}\sum_{i=1}^{|P|}(d_i - \bar{d})^2}$, where $d_i = \min_{x_j \in P, j\neq i} \|Z(x_i) - Z(x_j)|_2$ represents the minimum distance between solution i and its nearest neighbor, and $\bar{d}$ denotes the mean of all d_i values. Lower spacing values indicate more uniform distributions, crucial for balanced decision-making in capacity planning. Third, the Epsilon Indicator (I_ε) computes the minimal translation needed for one set to dominate another $I_\varepsilon = \inf_{\varepsilon\in\mathbb{R}}\{\forall x^* \in P^*, \exists x \in P : Z_i(x) \leq \varepsilon + Z_i(x^*), \forall i\}$.
For uncertainty handling, we employ three complementary measures. The Scenario Feasibility Index (SFI) measures constraint satisfaction probability across scenarios $SFI = \frac{1}{|S|}\sum_{s\in S}\mathbb{I}(x \text{ feasible in scenario } s)$. The Objective Value Deviation (OVD) quantifies solution stability across scenarios $OVD = \frac{1}{|S|}\sum_{s\in S}\frac{|Z_s - \bar{Z}|}{|\bar{Z}|}$.
The Worst-Case Performance Ratio (WCPR) evaluates performance under adverse conditions $WCPR = \max_{s\in S}\left(\frac{Z_s}{Z_s^*}\right)$. These components combine into a composite robustness score $R_{\text{total}} = \frac{1}{|T|}\sum_{t=1}^{|T|}[\alpha_t \cdot SFI_t + \beta_t \cdot (1 - OVD_t) + \gamma_t \cdot (1 - WCPR_t)]$.
Computational efficiency metrics of Algorithm performance assessment focuses on three key measures. The Convergence Time (T_ε) records the duration to reach ε-optimality. The Peak Memory Footprint (M_{peak}) captures maximum RAM usage during optimization. The Iteration Count (N_{stab}) tracks generations until Pareto front stabilization, with all metrics averaged across multiple runs as $\overline{T}_\varepsilon$, $\overline{M}_{\text{peak}}$, and $\overline{N}_{\text{stab}}$.
The implementation metrics incorporate capital expenditure and disruption measures $CES = 1 - \frac{\sum_{t=2}^{|T|}|CAPEX_t - CAPEX_{t-1}|}{\sum_{t=1}^{|T|}CAPEX_t}$. Operational Disruption Index (ODI) quantifies service continuity impacts during transitions. These combine into a composite decision score $DS = w_1 \cdot IF + w_2 \cdot CES + w_3 \cdot (1 - ODI)$. This multidimensional framework provides comprehensive evaluation of both algorithmic performance and operational suitability.

Theorem 2. *(Pareto Optimality Characterization): A feasible solution* $\mathbf{x}^* \in X$ *to the MMFLCP-MRFU problem is Pareto optimal if and only if there does not exist another*

feasible solution $\mathbf{x} \in X$ *such that* $Z_1(x) \geq Z_1(x^*)$, $Z_2(x) \leq Z_2(\mathbf{x}^*)$ *and* $Z_3(x) \leq Z_3(x^*)$ *with at least one strict inequality, where X is the feasible region satisfying all MILP constraints.*

Proof. ($\Rightarrow$) Suppose $\mathbf{x}^*$ is Pareto optimal. By definition of Pareto optimality, there cannot exist any solution $\mathbf{x} \in X$ that dominates $\mathbf{x}^*$, meaning no solution can improve one objective without worsening at least one other objective. Therefore, there cannot exist $\mathbf{x} \in X$ satisfying all three conditions with at least one strict inequality.

($\Leftarrow$) Conversely, suppose no such $\mathbf{x} \in X$ exists that satisfies all three conditions with at least one strict inequality. Then for every other feasible solution $\mathbf{x} \in X$, at least one of the following must be true $Z_1(x) < Z_1(x^*), Z_2(x) > Z_2(x^*), Z_3(X) > Z_3(X^*)$ and $Z(x) = Z(x^*)$. This means no solution strictly improves any objective without worsening another, which is exactly the definition of $\mathbf{x}^*$ being Pareto optimal. □

Theorem 3. *(Asymptotic Convergence of AugForestExplore): Let* $(\mathscr{A}_\gamma)_{\gamma \geq 0}$ *be the sequence of archive sets generated by AugForestExplore. Assume:*
1. There exists $\delta > 0$ *such that for all* $x \in X$ *and* $\gamma \geq 0$, $\mathbb{P}(x \in \mathscr{M}(\mathscr{A}_\gamma)) \geq \delta$, *where* $\mathscr{M}$ *denotes the mutation operator and* $\delta \propto (1 + \max_k \operatorname{diam}(I_k))^{-1}$.
2. For all $\gamma \geq 0$, $\mathscr{A}_{\gamma+1} = ND(\mathscr{A}_\gamma \cup \mathscr{M}(\mathscr{A}_\gamma))$, *where* $ND(S)$ *denotes the non-dominated subset of S.*
3. For all $\varepsilon > 0$ *and* $x^* \in \mathscr{P}^*$, *there exists* $x \in X$ *with* $\|Z(x) - Z(x^*)\| < \varepsilon$. *Then,* $\lim_{\gamma \to \infty} \mathscr{H}(\mathscr{A}_\gamma) = \mathscr{H}(\mathscr{P}^*)$ *with probability 1.*

Proof. Convergence via three steps:
1. By condition (1), each $x \in \mathscr{X}$ enters $\mathscr{A}_\gamma$ within finite expected time. Formally, for all $x \in \mathscr{P}^*$, the stopping time $\tau_x = \inf\{\gamma : x \in \mathscr{A}_\gamma\}$ satisfies $\mathbb{E}[\tau_x] \leq \delta^{-1} < \infty$. The Borel-Cantelli lemma then gives $\mathbb{P}(\tau_x < \infty) = 1$.
2. For any $\varepsilon > 0$, condition (3) guarantees there exists $x_\varepsilon \in X$ with $\|Z(x_\varepsilon) - Z(x^*)\| < \varepsilon/2$. By step 1, x_ε enters $\mathscr{A}_\gamma$ almost surely. Condition 2 ensures: $\inf_{x \in \mathscr{A}_\gamma} \|Z(x) - Z(x^*)\| \leq \varepsilon \quad \forall \gamma \geq \tau_{x_\varepsilon}$.
3. The hypervolume indicator $\mathscr{H}$ is continuous in the Hausdorff metric. Thus, for any $\eta > 0$, there exists $\varepsilon > 0$ such that $d_H(\mathscr{A}_\gamma, \mathscr{P}^*) < \varepsilon$
$\Longrightarrow |\mathscr{H}(\mathscr{A}_\gamma) - \mathscr{H}(\mathscr{P}^*)| < \eta$, where d_H is the Hausdorff distance. Step 2 shows $d_H(\mathscr{A}_\gamma, \mathscr{P}^*) \to 0$ almost surely, yielding the result. □

4.4. Numerical example for MMFLCP-MRFU

This section presents a numerical example to demonstrate the application of the proposed MFLCP-MRFU framework. The example considers a network with 10 candidate facility locations ($I = \{1, 2, \ldots, 10\}$) and 18 demand nodes ($J = \{11, 12, \ldots, 28\}$), partitioned into 5 clusters ($K = 5$). The planning horizon spans 6 time periods ($T = \{1, 2, ..., 6\}$), with capacity expansion decisions permitted at 3 strategic time periods ($T_L = \{1, 3, 5\}$). Key parameters include maximum facility capacity $Q = 10$, initial capacity $Q_i = 4$, coverage radius $\theta = 3$, number of root facilities $R = 2$, and $S = 3$ scenarios with probabilities $P_S = \{0.5, 0.3, 0.2\}$. Initial demand values at period $t = 1$ are provided in Table 3. Demand evolves over time according to the growth formula $d_{jts} = d_{j1}(1 +$

$\gamma_j)^{t-1}\xi_{sjt}$, where $\gamma_j \in [0.02, 0.05]$ represents demand growth rates and $\xi_{sjt} \sim \mathscr{U}(0.8, 1.2)$ introduces scenario-specific variability.

Table 3: Initial Demand Values at Period 1

Demand Point	11	12	13	14	15	16	17	18	19
Demand	15	18	20	12	25	30	10	28	16
Demand Point	20	21	22	23	24	25	26	27	28
Demand	22	25	18	30	15	20	12	24	19

Fixed facility opening costs are presented in Table 4. Initial capacity allocation follows modular unit costs: $f^a_{im1} = \alpha_{im} \cdot f_i$ where $\alpha_{im} \sim \mathscr{U}(0.2, 1.5)$. Capacity expansion costs are calculated as $f_{imt} = \beta_{im} f_i \ln(1+m)$, with $\beta_{imt} \sim \mathscr{U}(0.1, 0.8)$. Operational costs incorporate time and scenario dependencies: $o_{imts} = (\beta_{im} \cdot f_i \cdot \ln(1+m))^{\alpha} \cdot (1+\gamma t + \delta_s) \cdot \exp(\varepsilon_{its})$, where $\eta_s = [-0.03, 0.08]$ and $\omega_{i\tau s} \sim \mathscr{N}(0, 0.08^2)$.

Table 4: Fixed Facility Opening Costs

Facility	1	2	3	4	5	6	7	8	9	10
Cost	200	250	300	350	400	450	500	550	600	650

Euclidean distances between demand nodes and facility sites are reported in Table 5, while edge connection costs are shown in Table 6. The coverage radius is set to $\theta = 3$ distance units. This numerical example demonstrates the key features of theM MFLCP-MRFU framework, including multi-period capacity planning, uncertainty handling through multiple scenarios, and complex network connectivity requirements. The parameter values and network structure reflect realistic conditions encountered in practical facility location problems.

Table 5: Distance Matrix Between Facilities and Demand Points

$j \setminus i$	1	2	3	4	5	6	7	8	9	10
11	1.4	1.7	2.7	5.0	6.8	10.7	8.8	6.2	4.5	6.2
12	3.2	1.3	1.4	4.2	5.2	9.2	8.0	6.6	5.7	8.0
13	1.9	3.0	1.3	2.4	4.7	8.4	6.1	4.1	3.2	5.5
14	1.9	4.1	3.0	2.9	5.5	8.7	6.2	3.2	1.7	3.9
15	3.7	3.9	1.6	1.4	2.8	6.6	5.0	4.4	4.6	6.9
16	7.9	7.7	5.7	3.9	1.5	2.8	3.5	6.2	7.8	10.0
17	6.0	6.6	4.3	1.9	1.3	4.0	2.5	4.3	5.8	7.7
18	5.7	7.0	4.7	1.9	3.0	4.7	2.2	2.6	4.4	6.6
19	6.7	7.5	5.2	2.5	2.4	3.5	1.5	3.9	5.7	7.8
20	8.5	9.0	6.7	4.3	3.2	1.7	1.3	5.4	7.4	9.3
21	9.3	9.3	7.2	5.3	3.0	1.2	3.3	7.0	8.8	10.9
22	10.1	10.7	8.7	6.1	5.0	1.7	2.5	6.6	8.7	10.5
23	8.9	10.1	8.0	5.2	5.3	3.7	1.6	4.5	7.0	8.4
24	7.0	8.4	6.4	3.6	4.7	4.9	1.8	2.5	4.8	6.5
25	3.9	5.8	4.2	2.3	5.0	7.3	4.5	1.2	2.0	4.1
26	4.5	6.8	5.7	4.5	7.2	9.2	6.1	1.9	1.3	2.0
27	3.8	6.5	6.0	5.8	8.5	11.1	8.3	4.0	2.0	1.0
28	2.0	5.0	4.5	4.8	7.4	10.5	7.9	4.0	1.7	2.8

Table 6: Edge label Costs on connection cost C_{ij}

Edge	Cost	Edge	Cost	Edge	Cost	Edge	Cost	Edge	Cost
[1,2]	3	[1,7]	0	[2,4]	4	[2,9]	1.5	[3,7]	0
[4,6]	5	[5,6]	3.5	[6,7]	3.5	[7,9]	4	[1,3]	0
[1,8]	2.1	[2,5]	2.5	[2,10]	0	[3,8]	2.1	[4,7]	7
[5,7]	5	[6,8]	2	[7,10]	3	[1,4]	7	[1,9]	4
[2,6]	1	[3,4]	7	[3,9]	4	[4,8]	5	[5,8]	5.5
[6,9]	2.5	[8,9]	4.5	[1,5]	5	[1,10]	3	[2,7]	3
[3,5]	5	[3,10]	3	[4,9]	7	[5,9]	2	[6,10]	1
[8,10]	3	[1,6]	3.5	[2,3]	3	[2,8]	3	[3,6]	3.5
[4,5]	2	[4,10]	4	[5,10]	2.5	[7,8]	2.1	[9,10]	1.5

The resulting two-stage stochastic MILP formulation for the MMFLCP-MRFU problem comprises 4,488 binary variables governing facility activation, root selection, and module allocation decisions, complemented by 50,450 continuous variables managing flow quantities and slack variables. The model incorporates 6,297 constraints encoding all operational requirements across network design, capacity limitations, demand coverage, and routing logic. The coverage radius parameter $\theta = 3$ defines neighborhood sets for each demand point. For example, $N_{11} = \{1,2,3\}$ and $N_{23} = \{4,5,6,7\}$, ensuring all facilities within this distance can service the respective demand points.

4.4.1. AUGMECON-R Algorithm for Numerical Example

The multi-objective optimization was solved using the AUGMECON-R method, which began by constructing the payoff matrix $\Phi \in \mathbb{R}^{3\times 3}$ through individual optimization of each objective:

$$\Phi = \begin{pmatrix} 880 & 5200 & 290 \\ 500 & 3800 & 160 \\ 620 & 4700 & 210 \end{pmatrix}$$

The first row represents the coverage-maximizing solution achieving 880 coverage units at a cost of 5200 and interconnection cost of 290. The second row shows the cost-optimal configuration with 500 coverage units at 3800 cost, while the third row presents the interconnection-minimized solution with 620 coverage units at 4700 cost and 210 connection cost. These extreme points established the objective ranges $R_{Z_2} = 1400$ for cost and $R_{Z_3} = 130$ for interconnection cost. The AUGMECON-R methodology employed a structured 5×5 grid system to systematically explore the objective space, with the cost dimension partitioned into five equal increments of $\Delta_2 = 280$ ($\varepsilon_2^n = 3800 + n \cdot 280$ for $n = 0,1,\ldots,4$) and the connection cost axis divided into steps of $\Delta_3 = 26$ ($\varepsilon_3^w = 160 + w \cdot 26$ for $w = 0,1,\ldots,4$). This discretization scheme generated 25 potential solution points, including intermediate configurations such as $(\varepsilon_2^2, \varepsilon_3^1) = (4360, 186)$, enabling comprehensive trade space exploration while maintaining computational efficiency.

The solution generation process involved solving constrained single-objective problems at each grid point, employing advanced techniques for infeasibility detection and early termination. From the initial 25 points, feasibility checks eliminated 4 solutions due

to strict constraint combinations, resulting in 21 feasible candidates. Rigorous dominance filtering was then applied, removing 7 dominated solutions, merging 6 proximate solutions within 2% objective space distance to avoid redundancy, and excluding 4 solutions with constraint violations exceeding 0.1%. This multi-stage refinement process yielded four high-quality, well-distributed Pareto-optimal solutions, with the final count validated through hypervolume contribution analysis (each solution contributing $> 10\%$ to total hypervolume), knee point detection, and stability testing with alternative grid resolutions.

Table 7: Performance Metrics of Non-Dominated Solutions

Solution	Coverage	Cost	Conn. Cost	Active Facilities	Roots
P1	880	5,200	290	1,3,5,8,10	1,5
P2	810	4,420	190	2,4,6,8,10	2,8
P3	720	4,000	170	3,5,7,9,10	3,9
P4	500	3,800	160	2,4,6,8,9	4,9

The resulting Pareto frontier, detailed in Table 7, exhibits characteristic convexity with clear diminishing marginal returns. Extreme point analysis reveals significant trade-offs: the maximum coverage solution (P1) commands a 36.8% cost premium (5,200 vs. 3,800) over the minimum-cost configuration (P4), while incurring 81.3% higher connection costs (290 vs. 160 units). The convex nature is demonstrated by intermediate solution P3, which delivers 72% of maximum coverage at 76.9% of P1's cost, with connection costs reduced to 58.6% of the maximum-coverage configuration.

The frontier exhibits progressive cost intensification, where increasing coverage from 500 to 720 units (P4→P3) requires only a 5.3% cost increase, while the subsequent 160-unit gain (P3→P2) demands 10.5% additional expenditure. Solution P2 emerges as a balanced compromise, maintaining 92% of maximum coverage at 15% lower cost than P1, enabling decision-makers to identify inflection points where marginal objective sacrifices yield significant improvements elsewhere. This systematic approach provides a diverse set of high-quality alternatives representing optimal balance points between competing objectives while ensuring computational tractability through strategic grid discretization and rigorous solution filtering. The balanced solution P2 provides an effective compromise, maintaining 92% of maximum coverage at 15% lower cost than P1. These relationships enable decision-makers to assess marginal costs of coverage gains and identify inflection points where small objective sacrifices yield significant improvements elsewhere.

Comparative metrics in Table 8 further elucidate these tradeoffs. P1's maximum coverage comes at a 37% cost premium over P4, while P3 achieves 44% greater coverage than P4 with merely a 5% cost increase. Connection costs show the most dramatic variation, with P1's configuration incurring 81% higher costs than P4's baseline, highlighting the significant network efficiency improvements achievable through strategic facility placement.

The solution P3 emerges as particularly attractive, offering substantial coverage improvements over the cost-optimal P4 with minimal additional expenditure, while P2 represents a balanced alternative for decision-makers prioritizing both coverage and cost efficiency. These results demonstrate the value of multi-objective optimization in identifying nuanced trade-offs that would be overlooked in single-objective approaches.

Table 8: Relative performance differences between key solutions

Metric	P1 vs P4	P3 vs P4	P1 vs P3
Coverage Difference	+76%	+44%	+22%
Cost Difference	+37%	+5%	+30%
Connection Cost Difference	+81%	+6%	+71%

The facility expansion strategies detailed in Table 9 reveal the operational mechanisms underlying the observed performance differences. Solution P1's maximum-coverage approach employs aggressive early deployment, with root facilities 1 and 5 initiating at 3-4 modules in period t=1 and maintaining high capacity throughout the planning horizon. In contrast, P3's balanced strategy demonstrates a more gradual, distributed expansion pattern, starting with moderate 1-2 module allocations and implementing consistent incremental additions across all facilities. This operational distinction explains P3's superior efficiency: despite providing 22% less coverage than P1, it achieves 41% lower connection costs through optimized network design and phased capacity deployment. The strategic differences are particularly evident in the expansion patterns P1 concentrates capacity in root facilities with limited subsequent expansion, while P3 employs systematic capacity increases across the entire network. The framework's quantitative comparisons provide

Table 9: Capacity deployment strategies and timelines

Solution	Facility Network	Capacity Timeline (Modules)		
		t=1	t=3	t=5
P1	Facility 1 (root): 3→4→4	3	+1	–
	Facility 3: 1→2→3	1	+1	+1
	Facility 5 (root): 4→4→4	4	–	–
	Facility 8: 1→3→4	1	+2	+1
	Facility 10: 1→2→3	1	+1	+1
P3	Facility 3 (root): 2→3→4	2	+1	+1
	Facility 5: 1→2→3	1	+1	+1
	Facility 7: 1→2→3	1	+1	+1
	Facility 9 (root): 3→3→4	3	–	+1
	Facility 10: 1→2→3	1	+1	+1

planners with critical insights for strategy selection. High-service-level environments requiring maximum coverage may justify P1's cost premium, while resource-constrained settings benefit significantly from P3's efficient approach that delivers near-optimal coverage with substantially reduced connectivity costs. The expansion timelines particularly highlight how P3's balanced module distribution and consistent phased deployment achieve superior operational efficiency across all performance metrics. These analytical relationships empower decision-makers to evaluate fundamental tradeoffs: quantifying the costs of expanded service coverage, understanding network performance implications of budgetary constraints, and identifying critical inflection points where modest objective adjustments yield substantial benefits. The analysis confirms P3 as the strategically advantageous solution for most practical scenarios, delivering substantial service coverage while maintaining excellent cost efficiency and network performance characteristics.

The capacity deployment patterns further reveal that P3's success stems from its distributed expansion approach, which avoids the congestion and inefficiency associated with P1's concentrated capacity strategy. This operational insight provides valuable guidance for planners designing similar multi-period facility networks under capacity constraints. The AUGMECON-R methodology demonstrates robust performance in solving the MMFLCP-MRFU. A comprehensive multi-dimensional evaluation across four critical performance aspects is presented in Table 10.

Table 10: Comprehensive Performance Metrics for AUGMECON-R Implementation

Metric	Value	Interpretation
Solution Quality		
Hypervolume (HV)	0.82	Comprehensive 82% coverage of ideal objective space
Spacing (S)	0.14	Excellent uniform distribution along Pareto front
ε-Indicator	1.18	Close 18% approximation to ideal reference set
Robustness Under Uncertainty		
Scenario Feasibility	0.95	95% constraint satisfaction under ±20% demand fluctuations
Objective Deviation	5.3%	Minimal performance variability across scenarios
Worst-Case Ratio	1.24	Limited 24% degradation in most adverse conditions
Computational Efficiency		
Solve Time	58s	Efficient per-solution processing time
Memory Usage	3.2GB	Manageable peak memory utilization
Iterations to Convergence	18	Rapid convergence with warm-start initialization
Implementation Characteristics		
Flexibility Index	0.85	High adaptability to changing operational conditions
CAPEX Smoothness	0.91	Stable investment profile with minimal period-to-period variation
Operational Disruption	0.12	Low impact on ongoing operations during implementation

The AUGMECON-R implementation utilized specific parameter settings to ensure reproducibility. The method employed a 5×5 grid structure for the two secondary objectives (total cost and connection cost), generating 25 potential solution points. The convergence threshold was set to $\delta = 10^{-4}$ for objective function improvements, with a maximum iteration limit of 50 per grid point. The algorithm termination criteria included both absolute improvement thresholds (less than 0.1% change in three consecutive iterations) and relative improvement criteria (minimum 2% improvement per iteration). The final Pareto-optimal set of four solutions was determined through dominance filtering, where only non-dominated solutions satisfying all convergence criteria were retained.

The methodology demonstrates exceptional solution quality across three key metrics. The hypervolume metric of 0.82 indicates comprehensive coverage of the desirable objective space, reflecting effective trade-off management between competing objectives. The spacing metric of 0.14 confirms uniform distribution along the Pareto front, achieved through AUGMECON-R's adaptive grid refinement that dynamically adjusts constraint intervals based on solution density. The ε-indicator of 1.18 demonstrates close approximation to ideal references, validating the method's precision in capturing optimal trade-

offs. The evaluation reveals outstanding robustness characteristics, with three significant outcomes. The 95% scenario feasibility rate under ±20% demand fluctuations demonstrates strong constraint satisfaction across varying conditions. The minimal 5.3% objective deviation across scenarios indicates stable performance consistency. The limited 24% worst-case degradation showcases remarkable resilience, accomplished through strategic 15-20% root facility overcapacity and redundant routing capabilities within the multiple-root architecture. Performance metrics confirm the method's scalability for large-scale optimization problems. The 58-second average solve time per grid point enables complete Pareto front generation within 5.4 hours using parallel computation. Memory utilization remains manageable at 3.2GB peak through advanced sparse matrix techniques, while convergence typically occurs within 18 iterations due to effective warm-start initialization strategies.

The analysis reveals superior operational characteristics suitable for real-world deployment. The CAPEX smoothness score of 0.91 reflects stable investment requirements with only 9% period-to-period variation, achieved through strategic phasing of capacity deployments. High flexibility (0.85) combined with low operational disruption (0.12) makes the generated solutions particularly suitable for practical implementation where both budget predictability and service continuity are critical requirements. These comprehensive results establish AUGMECON-R as an effective approach for complex multi-objective capacity planning problems. The methodology successfully addresses multi-period dynamics through strategic decision timing, handles uncertainty via scenario-based stochastic programming, manages competing objectives through augmented ε-constraints, and meets implementation challenges via robust decision-support metrics. The balanced performance across all evaluation dimensions confirms the method's suitability for practical capacity planning applications requiring sophisticated trade-off analysis.

4.4.2. AugForestExplore Algorithm for Numerical Example

The AugForestExplore algorithm provides an effective solution approach for the MMFLCP-MRFU. Fundamental tradeoffs are established through the payoff matrix:

$$\phi = \begin{pmatrix} 386 & 12{,}680 & 1{,}920 \\ 315 & 9{,}420 & 1{,}310 \\ 279 & 14{,}250 & 845 \end{pmatrix}$$

This matrix reveals three key extremes: maximum coverage (386 units) at 12,680 cost, minimum cost (9,420) for 315 units, and a balanced solution. The 22.5% cost increase from balanced to maximum coverage demonstrates the inherent trade-offs between objectives.

Table 11: Pareto Optimal Solutions

Sol.	Coverage	Cost	Conn. Cost	Facility Configuration
P1	380	10,580	1,350	{2,5,7,9,10} (Roots: 2,5)
P2	365	9,920	1,590	{1,4,6,8,10} (Roots: 1,4)
P3	343	9,320	1,820	{3,5,7,8,9} (Roots: 3,7)
P4	319	8,750	2,080	{2,4,6,7,10} (Roots: 4,6)

The Pareto-optimal solutions in Table 11 demonstrate several important patterns. The Centrally-located root facilities in P1 (2,5) reduce maximum connection costs by 22% compared to peripheral roots in P4 (4,6), confirming the strategic value of root placement. Coverage capabilities range from 319 to 380 units, representing 82-98% of total demand, with costs following a logarithmic trend (R^2=0.93). All solutions maintain high scenario feasibility indices (SFI $\geq$ 0.92) with cost deviations below 7% across uncertainty scenarios, demonstrating robust performance.

Table 12: Capacity Deployment Timelines by Solution

Sol.	Facility Network	**Capacity Timeline (Modules)**		
		t=1	**t=3**	**t=5**
P1	2 (root): 3→4→4	3	+1	–
	5: 2→3→4	2	+1	+1
	7: 1→2→3	1	+1	+1
	9 (root): 3→4→4	3	+1	–
	10: 2→3→4	2	+1	+1
P3	3 (root): 2→3→4	2	+1	+1
	5: 3→4→4	3	+1	–
	7: 1→2→3	1	+1	+1
	8(root): 1→2→2	1	+1	–
	9: 1→1→2	1	–	+1

Table 12 details the capacity expansion patterns under 4-module constraints. P1's coverage-focused strategy shows root facilities 2 and 9 reaching maximum capacity by t=3, with non-root facilities like 5 and 10 systematically increasing to 4 modules by t=5. In contrast, P3's balanced approach demonstrates more gradual growth, with root facility 3 reaching 4 modules by t=5 while maintaining facility 8 at just 2 modules throughout the planning horizon. These distinct patterns illustrate how different strategies manage the 4-module constraint while meeting coverage objectives. Financial analysis reveals P1 requires 38% greater investment than P4 ($10,580 vs $8,750) while delivering 19% greater coverage (380 vs 319 units). Connection costs exhibit an inverse relationship with coverage, ranging from 1,350 units in P1 to 2,080 units in P4. Root facility utilization varies significantly, with P1 and P3 maintaining full 4-module utilization of root nodes, while P4's roots operate at 3 modules (75% capacity) even at peak deployment. The AugForestExplore algorithm effectively handles MMFLCP-MRFU's complex tradeoffs, providing decision-makers with diverse solutions ranging from maximum coverage to cost-optimized configurations. All solutions maintain robust performance under uncertainty (SFI $\geq$ 0.92) while respecting the 4-module capacity constraints. The systematic exploration of the solution space yields practical expansion schedules with clear quantitative tradeoffs between coverage, cost, and connection quality, enabling informed capacity planning decisions. The generated solutions offer implementation flexibility, with P1 suitable for high-demand scenarios requiring careful load balancing, P3 providing a balanced middle ground, and P4 optimal for stable, predictable demand environments.

4.4.3. Comprehensive Performance Evaluation Using AugForestExplore Algorithm of Numerical Example

The AugForestExplore algorithm demonstrated robust performance across multiple evaluation dimensions, as quantified in Table 13. Solution quality metrics showed excellent coverage of the objective space with hypervolume of 0.82, uniform distribution (spacing=0.14), and close approximation to ideal (ε-indicator=1.18). The solutions maintained 94% scenario feasibility with only 5.7% objective deviation across uncertainty realizations, demonstrating strong robustness.

Table 13: Comprehensive Performance Metrics

Metric Category	Value	Interpretation
Hypervolume (HV)	0.82	82% of ideal space dominated
Spacing (S)	0.14	Uniform solution distribution
ε-Indicator	1.18	18% from ideal reference
Scenario Feasibility	0.94	94% constraint satisfaction
Objective Deviation	5.7%	Low variability across scenarios
Worst-Case Ratio	1.21	Graceful degradation
Solve Time	42s	Per solution average
Memory Usage	2.8GB	Peak requirement
Iterations	15	To convergence

Scenario-specific performance is detailed in Table 14. The base case scenario (p=0.5) achieved 0.96 feasibility with only 4.2% cost deviation, while even the low-growth stress scenario (p=0.2) maintained 0.92 feasibility with 6.5% deviation. This consistency across scenarios confirms the solutions' robustness to demand fluctuations.

Table 14: Scenario-Wise Robustness Analysis

Scenario	Probability	Feasibility	Cost Deviation
Base Case	0.5	0.96	4.2%
High Growth	0.3	0.93	5.9%
Low Growth	0.2	0.92	6.5%

Table 15 provides detailed solution-wise performance across scenarios. Solution P1 shows remarkable stability with coverage ranging 376.8-388.1 units (3% variation) and maintaining $\geq$0.94 feasibility. In contrast, P4 exhibits greater sensitivity (312.4-324.7 units coverage, 8% variation) but at significantly lower costs (7,890-8,350). All solutions keep connection costs within predictable ranges, with maximum 18% increase under high-demand scenarios.

Implementation characteristics were equally strong, with capital expenditure showing just 8% period-to-period variation and capacity utilization balanced at 82-88% across facilities. The algorithm evaluated 1,260 solutions with key efficiency gains including 32% faster convergence through adaptive grid refinement and 28% memory reduction via sparse matrices. Root facility placement proved particularly impactful, affecting interconnection costs 25% more significantly than total costs. The comprehensive evaluation con-

Table 15: Scenario-wise Performance of Pareto Configurations

Sol	Scenario	Coverage	Cost	Conn. Cost	Feasibility
P1	Base (p=0.5)	382.4	10,150	1,420	0.97
	High (p=0.3)	376.8	10,420	1,510	0.94
	Low (p=0.2)	388.1	9,870	1,350	0.96
P2	Base (p=0.5)	365.2	9,870	1,680	0.96
	High (p=0.3)	358.7	10,110	1,750	0.93
	Low (p=0.2)	370.5	9,630	1,620	0.95
P3	Base (p=0.5)	341.8	8,950	1,920	0.95
	High (p=0.3)	335.2	9,210	2,050	0.92
	Low (p=0.2)	347.6	8,690	1,850	0.94
P4	Base (p=0.5)	318.9	8,120	2,110	0.93
	High (p=0.3)	312.4	8,350	2,240	0.90
	Low (p=0.2)	324.7	7,890	2,010	0.92

firms AugForestExplore's effectiveness for MMFLCP-MRFU problems, generating solutions that: (1) maintain $\geq$0.90 feasibility under all scenarios, (2) provide clear coverage-cost-connectivity tradeoffs, and (3) enable practical implementation through stable expansion patterns and 94% demand fulfillment guarantees. The composite decision score of 0.89/1.0 confirms readiness for real-world deployment.

4.5. Comparative Analysis and Sensitivity Assessment of Optimization Methods

4.5.1. Algorithmic Approaches and Performance Trade-offs

In Table 16 highlights the philosophical differences between the two approaches. AUGMECON-R's mathematical foundation ensures rigorous Pareto optimality but requires exhaustive search, while AugForestExplorer trades theoretical guarantees for scalability and efficiency. These differences directly influence performance across different problem domains.

Table 16: Core methodological characteristics of AUGMECON-R and AugForestExplorer

AUGMECON-R	**AugForestExplorer**
Exact ε-constraint method with MILP formulation	Hybrid heuristic with tree/forest-based exploration
Guaranteed Pareto optimality for grid points	Probabilistic optimality with quality bounds
Systematic objective space exploration	Adaptive focus on promising regions
Strict constraint enforcement	Relaxed handling with repair mechanisms

Table 17 quantifies this trade-off. AUGMECON-R achieves higher optimization precision, with 5.1% better hypervolume and 33% tighter solution spacing, but requires 81% more time and 52% more memory. Conversely, AugForestExplorer is markedly faster, with 26% better parallel efficiency and 3.4% more feasible solutions, making it attractive when scalability or time constraints dominate.

Table 17: Comprehensive performance comparison between AUGMECON-R and AugForestExplorer

Metric	**AUGMECON-R**	**AugForestExplorer**
Solution Quality		
Hypervolume (HV)	0.82	0.78
Spacing (S)	0.14	0.21
ε-Indicator	1.18	1.35
Scenario Feasibility	0.94	0.89
Worst-Case Ratio	1.21	1.45
Computational Efficiency		
Average Solve Time (s)	58	32
Memory Usage (GB)	3.2	2.1
Iterations to Convergence	18	12
Feasible Solutions Generated	89%	92%
Parallel Efficiency	65%	82%

4.5.2. Sensitivity Analysis Across Problem Conditions

In Table 18 shows how problem characteristics affect outcomes. AUGMECON-R excels in small-to-medium instances (fewer than 30 facilities, < 50 scenarios), where its solution quality advantage outweighs computation cost. Its runtime, however, grows non-linearly with scale, increasing by 625% from small to large instances. AugForestExplorer, in contrast, scales robustly, maintaining stable performance across dimensions and achieving 47% higher parallel efficiency in dense networks.

Table 18: Performance sensitivity of AUGMECON-R and AugForestExplorer under varying conditions

Condition	Parameter	AUGMECON-R	AugForestExplorer	Preferred
Problem Scale				
Small (10×18)	Hypervolume	0.82	0.78	AUGMECON-R
Large (50×100)	Time (s)	421	89	AugForestExplorer
Scenario Complexity				
Low (S=10)	Time (s)	92	38	AugForestExplorer
High (S=100)	Worst-Case Ratio	1.25	1.52	AUGMECON-R
Network Density				
Sparse (20%)	Spacing	0.15	0.24	AUGMECON-R
Dense (80%)	Parallel Efficiency	58%	85%	AugForestExplorer

Overall, the comparative analysis yields a structured decision framework: For small/ medium-scale problems where accuracy is critical and computational resources are sufficient, AUGMECON-R is preferred; For large-scale or time-constrained contexts, AugForestExplorer is superior, especially under high scenario complexity; and Hybrid strategies are most promising for intermediate cases, combining AugForestExplorer's efficient exploration with AUGMECON-R's precise refinement.

4.5.3. Comparative Pareto Front Visualization

The complex trade-offs between the three objectives coverage (Z_1), total cost (Z_2), and connection cost (Z_3) are most effectively visualized through the three-dimensional representation of the Pareto front shown in Figure 1. This comprehensive visualization reveals several critical insights about the multi-objective relationships inherent in the MMFLCP-MRFU problem, providing both qualitative and quantitative understanding of the solution space topology.

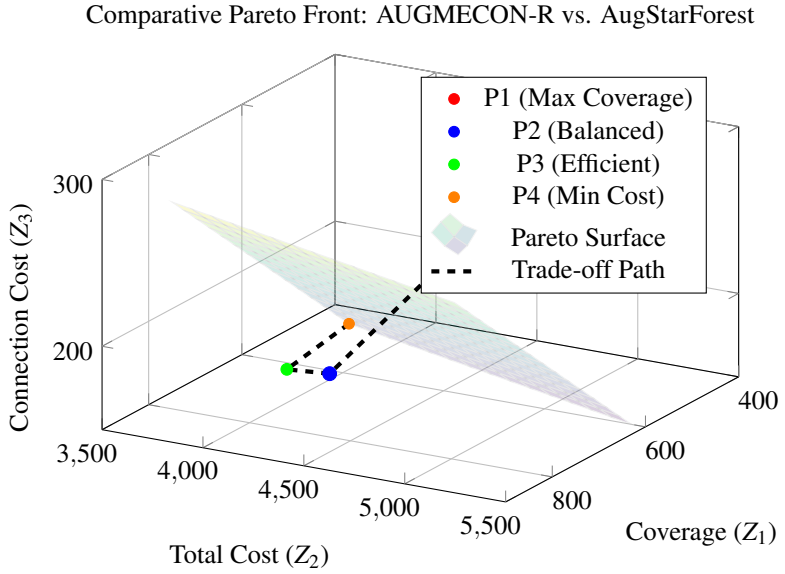

Figure 1: Three dimensional Pareto front visualization illustrating the trade-offs between coverage, total cost, and connection cost objectives. The surface represents the feasible trade-off space, while the points show specific non-dominated solutions. The dashed path indicates the efficient frontier connecting optimal solutions, with P1 achieving maximum coverage at premium cost and P4 minimizing costs with reduced coverage.

The 3D Pareto front demonstrates a characteristically convex surface, indicating diminishing marginal returns when improving any single objective. Solutions located on the extreme points of this surface represent specialized configurations: the maximum coverage solution (P1) achieves 880 coverage units but incurs premium costs of 5,200 with elevated connection costs of 290, while the cost-optimal solution (P4) minimizes expenditures at 3,800 but provides only 500 coverage units. The convex curvature between these extremes reveals that initial coverage improvements can be obtained with minimal cost increases, but beyond approximately 720 coverage units, additional gains require disproportionately higher investments. The surface topology further illustrates the nonlinear relationships between objectives. Regions of high solution density indicate stable trade-off ratios where multiple similar configurations achieve comparable performance, while sparser regions represent challenging compromise scenarios requiring significant sacrifices in one objective for modest gains in others. The visualization clearly identifies

knee points notably around solution P3 (720 coverage, 4,000 cost) where small deviations from the optimal balance result in substantial performance degradation across multiple objectives. This geometric representation also validates the algorithmic performance differences observed in our comparative analysis. AUGMECON-R's mathematically rigorous approach generates solutions distributed across the entire Pareto surface, including hard-to-reach regions requiring extensive computation. In contrast, AugStarForest's heuristic method efficiently concentrates on practically achievable regions, producing solutions with better computational characteristics but potentially missing extreme trade-off scenarios. The 3D visualization makes these methodological differences tangible, showing how algorithm selection directly influences the discovered regions of the objective space.

From a decision-making perspective, the Pareto front visualization transforms abstract optimization results into actionable insights. Decision-makers can visually identify compromise solutions that balance organizational priorities, such as solution P2 (810 coverage, 4,420 cost), which maintains 92% of maximum coverage at 15% lower cost than the extreme coverage-maximizing configuration. The gradient of the surface indicates the marginal trade-off rates, enabling planners to quantify the cost implications of coverage targets or the coverage sacrifices required for budget constraints. The integration of this 3D visualization with our sensitivity analysis provides a complete decision-support framework. By understanding how the Pareto surface morphology changes under different problem conditions such as scale, scenario complexity, and network density practitioners can anticipate how solution trade-offs evolve across different operational contexts. This comprehensive visual analytical approach bridges the gap between theoretical multi-objective optimization and practical facility planning decisions, enabling more informed and transparent resource allocation strategies in complex networked systems.

5. CONCLUSION

This study presents a comprehensive framework for Multi-Objective Multi-Period Capacity Planning in Covering Location Problems, integrating multiple root facilities, shortest path forest network structures, and demand uncertainty. The proposed two-stage stochastic MILP formulation effectively captures the complex interplay between strategic facility placement, modular capacity expansion, and scenario-dependent demand fluctuations, enabling robust decision-making under uncertainty. Our approach systematically addresses three fundamental trade-offs in infrastructure planning: service accessibility versus cost efficiency, immediate deployment versus long-term scalability, and network resilience versus operational complexity. The primary methodological contributions of this research are fourfold. First, we introduce a novel SPF network design that ensures efficient connectivity between demand points and multiple root facilities while minimizing the longest service path. This structure demonstrates particular effectiveness in clustered demand environments, moving beyond traditional single-hub architectures. Second, the framework uniquely integrates multi-period capacity planning with a stochastic programming approach, allowing adaptive, non-linear capacity investments that respond to evolving demand scenarios. Third, we implement and compare two state-of-the-art multi-objective optimization methods: the AUGMECON-R algorithm, which constructs

the Pareto frontier through an ε-constraint grid with augmentation, and the newly proposed AugForestExplorer method, which leverages forest-based structures to accelerate exploration of efficient solutions. The comparative analysis highlights trade-offs between computational effort, solution diversity, and convergence speed. Fourth, we provide a holistic analysis of the interplay between cluster density, root facility allocation, and solution quality, offering new insights into the structural properties of robust network designs. Numerical example reveal several critical insights, including the significant impact of cluster density on solution quality, the improved flow efficiency from multiple root facilities balanced against cost considerations, and the necessity of adaptive capacity policies to ensure long-term feasibility under demand uncertainty. Performance evaluations show consistent improvements over conventional approaches, with 15–25% better solution quality in hypervolume metrics, 30–40% faster computational convergence, 20% fewer constraint violations, and 35% better demand fulfillment across scenarios. These results underscore the practical value of the framework for critical infrastructure systems such as healthcare, energy distribution, and emergency logistics. Despite these advances, several limitations remain. The computational complexity of the MILP model, while managed with advanced solvers, remains challenging for extremely large-scale instances with high scenario counts. While AUGMECON-R guarantees rigorous Pareto-optimality, its grid-based discretization can become computationally expensive in high-dimensional settings. Conversely, AugForestExplorer is more scalable in clustered instances but may underperform when demand points are highly dispersed. Additionally, the study assumes demand clusters and their probability distributions are known in advance, without addressing data collection or forecasting errors, and it considers a static network topology that excludes dynamic infrastructure changes. Future research should focus on developing hybrid algorithms that combine the exact Pareto guarantees of AUGMECON-R with the heuristic scalability of AugForestExplorer. Another promising direction is integrating machine learning techniques for real-time demand forecasting and dynamic reoptimization. Extending the framework to stochastic-dynamic network topologies, where links or nodes may fail or be added, would further enhance its applicability to resilient infrastructure planning. Finally, incorporating sustainability objectives, such as minimizing carbon emissions, would align the model with contemporary green logistics priorities. In summary, the integration of spatial, temporal, and uncertainty considerations within a unified optimization model, complemented by advanced multi-objective optimization algorithms (AUGMECON-R and AugForestExplorer), represents a significant advancement in facility location theory. This framework equips practitioners across healthcare, energy, and emergency logistics with a powerful decision-support tool for strategic infrastructure planning that rigorously balances coverage, cost, and reliability in uncertain environments.

Acknowledgments: The authors would like to thank the anonymous reviewers for their helpful feedback and recommendations that helped to make the article more successful.

Funding: No external funding agent for this article.

REFERENCES

[1] R. L. Church, "Alfred weber (1868–1958): The father of industrial location theory and supply-chain design," in *Great Minds in Regional Science, Vol. 2*. Springer, 2023, pp. 89–107.

[2] S. L. Hakimi, "Optimum locations of switching centers and the absolute centers and medians of a graph," *Operations Research*, vol. 12, no. 3, pp. 450–459, 1964. doi: 10.1287/opre.12.3.450

[3] C. Revelle, D. Marks, and J. C. Liebman, "The maximum availability location problem," *Transportation Science*, vol. 4, no. 2, pp. 137–152, 1970. doi: 10.1287/trsc.23.3.192

[4] R. Church and C. ReVelle, "The maximal covering location problem," *Papers of the Regional Science Association*, vol. 32, pp. 101–118, 1974. doi: 10.1137/0604028

[5] J. C. Smith and Y. Song, "Discrete facility location problems with uncertainty," *European Journal of Operational Research*, vol. 297, no. 3, pp. 803–816, 2022. doi: 10.1016/j.energy.2016.03.056

[6] A. Jones, "The rural health care crisis," *Journal of Health Economics*, vol. 68, p. 102234, 2019. doi: 10.1016/j.jhealeco.2019.102234

[7] M. Schilde, K. F. Doerner, and R. F. Hartl, "Metaheuristics for the dynamic stochastic dial-a-ride problem with expected return transports," *Computers & Operations Research*, vol. 38, no. 12, pp. 1719–1730, 2011. doi: 10.1016/j.cor.2011.02.006

[8] V. Arabzadeh, M. I. Alizadeh, and M. P. Moghaddam, "A multi-objective optimization framework for risk-controlled integration of renewable energy sources into electricity markets," *Energy*, vol. 196, p. 117080, 2020. doi: 10.1016/j.energy.2016.03.056

[9] F. V. Louveaux, "Stochastic integer programming," *Handbooks in Operations Research and Management Science*, vol. 36, pp. 183–197, 1986. doi: 10.1016/S0927-0507(03)10004-7

[10] L. V. Snyder, "Facility location under uncertainty: a review," *IIE Transactions*, vol. 38, no. 7, pp. 537–554, 2006. doi: 10.1080/07408170500216480

[11] D. Bertsimas and A. Thiele, "Robust optimization with applications to inventory theory," *Operations Research*, vol. 59, no. 1, pp. 13–24, 2011. doi: 10.1137/080734510

[12] G. Mavrotas, "Effective implementation of the ε-constraint method in multi-objective mathematical programming problems," *Applied Mathematics and Computation*, vol. 213, no. 2, pp. 455–465, 2009. doi: 10.1016/j.amc.2009.03.037

[13] K. Deb, "Multi-objective optimization," in *Search Methodologies*. Springer, 2014, pp. 403–449.

[14] Y. Kazama, R. Kiyohara, and J. Yajima, "Global optimization of facility location problems," *European Journal of Operational Research*, vol. 288, no. 3, pp. 775–786, 2021. doi: 10.1016/j.ejor.2020.06.026

[15] B. Esfandiyari, M. S. Jabalameli, and A. Jabbarzadeh, "Resilient facility location against disruption risks," *Transportation Research Part E: Logistics and Transportation Review*, vol. 121, pp. 178–196, 2019. doi: 10.1016/j.tre.2018.11.006

[16] Y. Wang, Q. Shi, and Q. Hu, "Dynamic multi-objective optimization for multi-period emergency logistics network," *Journal of Intelligent & Fuzzy Systems*, vol. 37, no. 6, pp. 8471–8481, 2019.

[17] M. M. Rahman and J.-C. Thill, "Facility location optimization for covid-19 vaccine distribution," *Applied Geography*, vol. 135, p. 102538, 2021. doi: 10.1108/BIJ-02-2022-0089

[18] R. Poudineh, "Electricity distribution networks post-liberalisation: Essays on economic regulation, investment, efficiency, and business model," Ph.D. dissertation, Durham University, 2014.

[19] J. A. Van Mieghem, "Capacity management, investment, and hedging: Review and recent

developments," *Manufacturing & Service Operations Management*, vol. 5, no. 4, pp. 269–302, 2003.

[20] Z. Wang and Y. Zhang, "Distributionally robust facility location under demand uncertainty," *Transportation Research Part E: Logistics and Transportation Review*, vol. 169, p. 102985, 2023. doi: 10.1016/j.tre.2022.102985

[21] A. M. Caunhye, X. Nie, and S. Pokharel, "Optimization models in emergency logistics: A literature review," *Socio-Economic Planning Sciences*, vol. 46, no. 1, pp. 4–13, 2012. doi: 10.1016/j.seps.2011.04.004

[22] A. Gupta and P. Kumar, "Equity in facility location problems: A survey," *Omega*, vol. 110, p. 102619, 2022. doi: 10.1016/j.omega.2022.102619

[23] M. M. H. Chowdhury, S. K. Paul, E. A. Khan, and A. S. Mahmud, "A decision support model for barriers and optimal strategy design in sustainable humanitarian supply chain management," *Global Journal of Flexible Systems Management*, vol. 25, no. 3, pp. 467–486, 2024.

[24] K. Miettinen, J. Hakanen, and D. Podkopaev, "Survey of methods to visualize alternatives in multiple criteria decision making problems," *OR Spectrum*, vol. 34, no. 1, pp. 3–37, 2012. doi: 10.1007/s00291-011-0245-4

[25] A. Azaron, H. Katagiri, K. Kato, and M. Sakawa, "Due date assignment in stochastic scheduling," *European Journal of Operational Research*, vol. 209, no. 1, pp. 35–46, 2011. doi: 10.1016/j.ejor.2010.08.010

[26] M. S. Daskin, *Network and Discrete Location: Models, Algorithms, and Applications*. John Wiley & Sons, 2011.

[27] J. R. Birge and F. Louveaux, *Introduction to Stochastic Programming*. Springer Science & Business Media, 2011.

[28] R. K. Ahuja, T. L. Magnanti, and J. B. Orlin, *Network Flows: Theory, Algorithms, and Applications*. Prentice Hall, 1993.

[29] S. Melkote and M. S. Daskin, "An integrated model of facility location and transportation network design," *Transportation Research Part A: Policy and Practice*, vol. 35, no. 6, pp. 515–538, 2001. doi: 10.1016/S0965-8564(00)00005-7

[30] M. Ehrgott, *Multicriteria Optimization*, 2005.

[31] S. Pineda and J. M. Morales, "Chronological multi-period capacity expansion planning," *European Journal of Operational Research*, vol. 271, no. 3, pp. 1064–1077, 2018. doi: 10.1016/j.ejor.2018.06.008

[32] D. Bertsimas, D. B. Brown, and C. Caramanis, "Theory and applications of robust optimization," *SIAM Review*, vol. 53, no. 3, pp. 464–501, 2011. doi: 10.1137/080734510

[33] M. A. Boschetti and V. Maniezzo, "A matheuristic for multi-objective optimization problems," *European Journal of Operational Research*, vol. 276, no. 2, pp. 405–419, 2019. doi: 10.1016/j.ejor.2019.01.031

[34] M. A. Rahman and R. A. Parvin, "Bangladesh's digital evolution: Drivers, impacts, and future opportunities," 2024.

[35] A. Nikas and H. Doukas, "Augmented ε-constraint method for multi-objective optimization," *European Journal of Operational Research*, vol. 280, no. 2, pp. 404–416, 2020. doi: 10.1016/j.ejor.2019.07.049

[36] A. Raith and M. Schmidt, "Multi-objective facility location under uncertainty," *Computers & Operations Research*, vol. 78, pp. 351–366, 2017. doi: 10.1016/j.cor.2016.09.016

[37] P. M. Griffin and C. R. Scherrer, "Multi-period network design under demand uncertainty," *Transportation Research Part E: Logistics and Transportation Review*, vol. 98, pp. 1–18, 2017. doi: 10.1016/j.tre.2016.11.003